N71-13598

NASA CR 72759
GLR-84

SNAP-8 BOILER PERFORMANCE DEGRADATION AND
TWO-PHASE FLOW HEAT AND MOMENTUM
TRANSFER MODELS

by

H. F. Poppendiek

GEOSCIENCE LTD

prepared for

NATIONAL AERONAUTICS AND SPACE ADMINISTRATION

NASA Lewis Research Center
Contract NAS 3-11836
Edward R. Furman, Project Manager

NOTICE

This report was prepared as an account of Government-sponsored work. Neither the United States, nor the National Aeronautics and Space Administration (NASA), nor any person acting on behalf of NASA:

A.)   Makes any warranty or representation, expressed or implied, with respect to the accuracy, completeness, or usefulness of the information contained in this report, or that the use of any information, apparatus, method, or process disclosed in this report may not infringe privately-owned rights; or

B.)   Assumes any liabilities with respect to the use of, or for damages resulting from the use of, any information, apparatus, method or process disclosed in this report.

As used above, "person acting on behalf of NASA" includes any employee or contractor of NASA, or employee of such contractor to the extent that such employee or contractor of NASA or employee of such contractor prepares, disseminates, or provides access to any information pursuant to his employment or contract with NASA, or his employment with such contractor.

Requests for copies of this report should be referred to

National Aeronautics and Space Administration
Scientific and Technical Information Facility
P. O. Box 33
College Park, Md. 20740

TOPICAL REPORT

SNAP-8 BOILER PERFORMANCE DEGRADATION AND
TWO-PHASE FLOW HEAT AND MOMENTUM
TRANSFER MODELS

by

H. F. Poppendiek

GEOSCIENCE LTD
410 South Cedros Avenue
Solana Beach, California   92075

prepared for

NATIONAL AERONAUTICS AND SPACE ADMINISTRATION

August 1970

CONTRACT NAS 3-11836

NASA Lewis Research Center
Cleveland, Ohio
Edward R. Furman, Project Manager
SNAP-8 Project Office

TABLE OF CONTENTS

ABSTRACT

A discussion of boiler deconditioning phenomena and possible
causes are reviewed. Controlling heat transfer mechanisms
in connection with deconditioning are described, and the
results of analyses that define 4P3E oil transport, decom-
position and deposition in boiler tubes are summarized.

Heat transfer and fluid flow models that describe a number
of pertinent flow regimes and phase distributions are reca-
pitulated. Limitations and applicability criteria are also
presented for the models. In addition, a number of practical
questions relating to boiler design and performance are
considered.

SUMMARY

The results of the studies pursued in this program can be summarized briefly as follows:

1. Oil leakage into the SNAP-8 mercury circuit can be transported into the boiler by two-component annular flow.

2. Oil films in the boiler at design temperatures can be decomposed and the solid products deposited in the boiler.

3. Decomposed oil deposits (and oxide deposits during earth-based operations) can significantly increase droplet vaporization lifetimes, cause changes in phase distributions in the boiler tube and reduce the corresponding boiling conductances.

4. In order to guarantee no oil transport into the boiler, effective oil traps should be used in the systems.

5. The heat transfer and pressure drop performance of SNAP-8 boilers can be defined by a number of idealized flow models (annular flow, wetted wall rivulet flow, film boiling droplet flow, slug flow, and vapor flow).

6. Some approximate flow regime criteria have been developed which assist in defining which boiling regime is in operation.

I. INTRODUCTION

The design of mercury boilers for space power application is more difficult than that for water boilers. The relative distribution of the liquid and vapor phases for mercury flow (even in the earth's gravitational field) can be complex and varied depending upon the velocity field and the surface physics and chemistry at the inner wall of the boiler tube. Quantitative information is required on how the phases are distributed, what the corresponding heat transfer and pressure drop functions are and how the addition of impurities and deposits at the boiler tube wall change these quantities.

In 1967, Geoscience started a two-year study on boiler degradation and two-phase flow heat and momentum transfer under support by the SNAP-8 Project at the NASA-Lewis Research Center. The technical monitors were Messrs. E. R. Furman, G. M. Thur, and M. J. Saari. The scope of the work included 1) derivations of heat transfer and fluid flow equations applicable to specific SNAP-8 boiler inserts, 2) prediction of droplet vaporization lifetime functions accounting for boiler surface deposits and degree of wetting, 3) development of mathematical models that define 4P3E oil transport, decomposition and deposition in boiler tubes, 4) mercury droplet vaporization experiments with tantalum surface in controlled, gaseous environments, and 5) 4P3E oil transport, decomposition and deposition experiments.

This Topical Report recapitulates the important parts of the two Annual Reports[1,2] of the previous study. In addition, the heat and momentum transfer model results for circular cross-section tubes derived primarily from a previous study that Geoscience conducted for the AEC[3] (initiated in 1961) are utilized.

Valuable information was obtained from Aerojet on the experimental heat transfer and pressure drop performance including boiler degradation behavior for SNAP-8 boilers in full-scale systems. Comparisons between Geoscience's boiler performance predictions and experimental behavior are presented and discussed in some detail in an Aerojet report prepared by Mr. A. J. Sellers (NASA report CR 72760).

II. BOILER PERFORMANCE DEGRADATION

A. Description of Boiler Deconditioning Phenomena and Possible Causes

Boiler deconditioning is a term used to describe any degradation of boiler heat transfer and pressure drop characteristics. Consider the case where the liquid metal in a boiler is in good contact with the prime heat transfer surface (achieved by strong rotational fluid flow or by good wetting). If changes in surface chemistry or physics occur at the boiler tube wall, the wetting characteristics and liquid phase distribution change thereby modifying the heat transfer and pressure drop performance.

There are two known chemical contaminants that can exist at the boiler tube wall of a SNAP-8 system, namely, oxide deposits and decomposed oil deposits. Oxygen should only be able to get into the system during earth-based operation when system pressures momentarily fall below the environmental pressures and leaks exist; because this condition would not be present during space operation, it was felt that the oxide deposit question need not be given much attention[*]. Decomposed oil deposits can occur whenever oil seal leaks take place; the effects of this type of surface contamination is given major consideration in this report.

B. Boiler Deconditioning Mechanisms

A recapitulation of the experimental and analytical research results relating to and verifying the controlling boiler deconditioning mechanisms is given below.

Experimental Evidence
A series of mercury droplet vaporization experiments on tantalum surfaces (in argon gas and mercury vapor environments) were performed to determine the effects of surface physics and chemistry on droplet vaporization lifetimes, θ_ℓ, which are inversely proportional to boiling conductances. A diagram of the system is shown in Figure 1.

---

[*]In the event that the reader wishes to learn more about the oxidation question, reference 1 can be consulted wherein specific evidence of the effect of oxide formation on the inside of boiler tube walls on boiling heat transfer is presented.
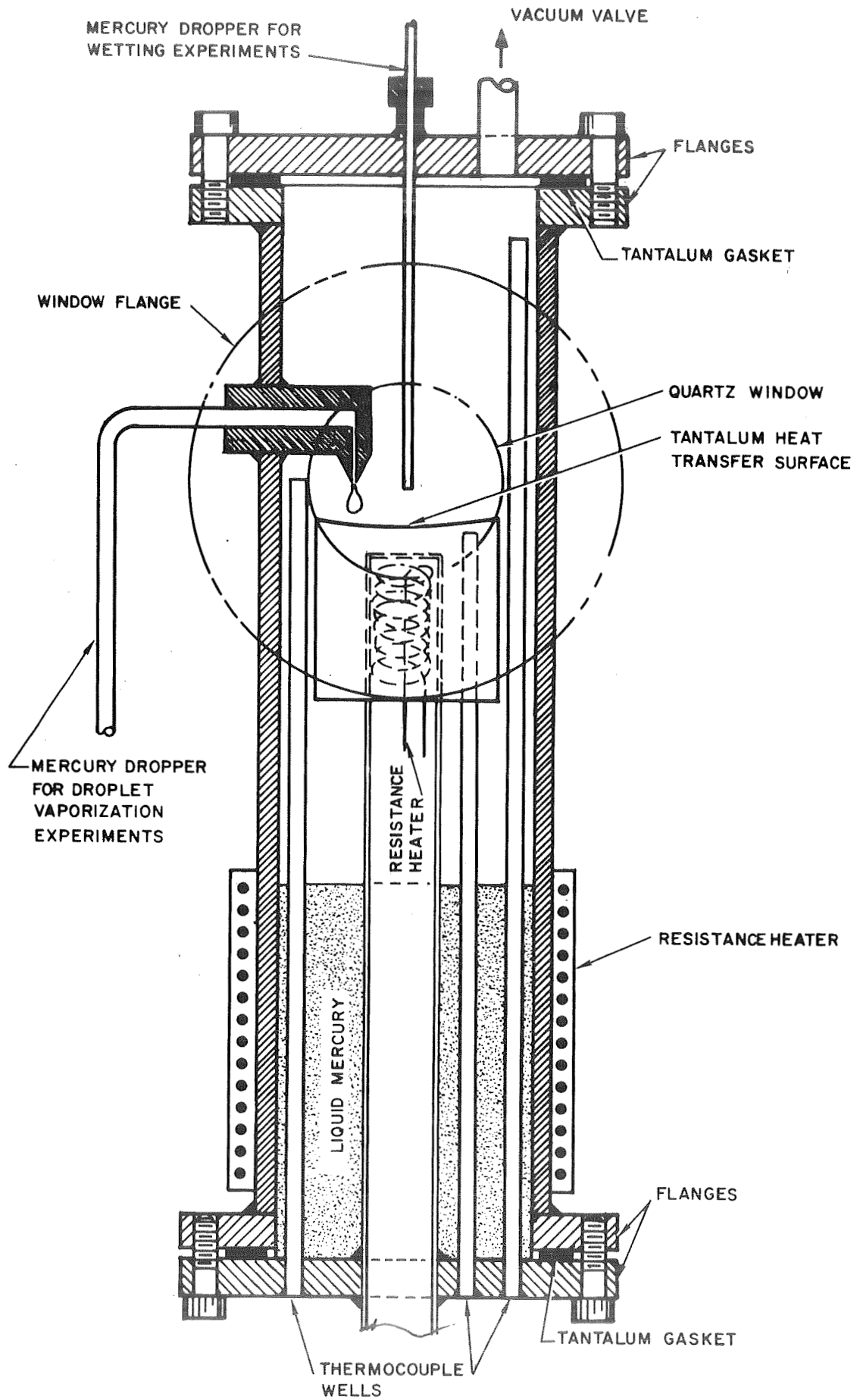
MERCURY DROPPER FOR
WETTING EXPERIMENTS

VACUUM VALVE

FLANGES

TANTALUM GASKET

WINDOW FLANGE

QUARTZ WINDOW

TANTALUM HEAT
TRANSFER SURFACE

MERCURY DROPPER
FOR DROPLET
VAPORIZATION
EXPERIMENTS

RESISTANCE HEATER

RESISTANCE HEATER

LIQUID MERCURY

FLANGES

TANTALUM GASKET

THERMOCOUPLE
WELLS

4

Figure 1. Droplet vaporization chamber.

The experiments made in an argon environment indicated that:

1)   Different chemical cleaning solution and cleaning procedures can produce lifetimes that differ as much as an order of magnitude during surface vaporization, $0 < (t_w - t_{sat}) < 100\,°F$, and transition boiling, $100 < (t_w - t_{sat}) < 300\,°F$ (see Figure 2).

2)   Surface oxidation can increase the lifetimes by as much as an order of magnitude in the surface vaporization region and the initial part of the transition region (see Figures 3 and 4, and Table I).

3)   Decomposed 4P3E oil films can increase lifetimes by an order of magnitude in the surface vaporization region, increase lifetimes by less than an order of magnitude in the initial part of the transition region and reduce lifetimes by as much as fifty percent in the latter part of the transition region (see Figure 5).

In addition to the droplet vaporization experiments in an argon environment, a special apparatus was used to make some lifetime measurements in an all-mercury vapor environment; time permitted the investigation of only a clean surface, however. In the range of interest for the SNAP-8 program, i.e., $\Delta t = 20\,°F$ or less, the lifetime values for the mercury vapor environment were similar to those measured in an argon environment (in the same apparatus). In the latter part of the surface vaporization region, the lifetimes for the mercury vapor environment were considerably higher than those for the argon environment (see Figure 6). It was not possible to give a complete interpretation of these limited data on the basis of the time and funding available for this part of the program. It is believed that in the surface vaporization region $(0 < \Delta T < 20\,°F)$, the controlling thermal resistance is in the liquid drop adhering to the heat transfer surface; thus, differences in evaporation resistances in argon and mercury vapor environments would not be important. In the transition and film boiling regions ($\Delta T > 20\,°F$), the controlling thermal resistances are more complicated. In these cases, the liquid drops are often separated from the boiler tube wall by the environmental gas. Probably the low thermal conductivity of mercury vapor (compared to the argon gas) accounts partly for the longer lifetimes in the mercury vapor environment for $\Delta T > 20\,°F$. Also, the increased partial pressure driving force in the evaporation equation for the argon gas environment case may account partly for the corresponding shorter lifetimes.

Special tantalum-mercury wetting experiments were also conducted in which the contact angle was measured in a saturated mercury vapor contained in a sealed quartz tube. The results indicated that chemically-clean, triple-distilled mercury
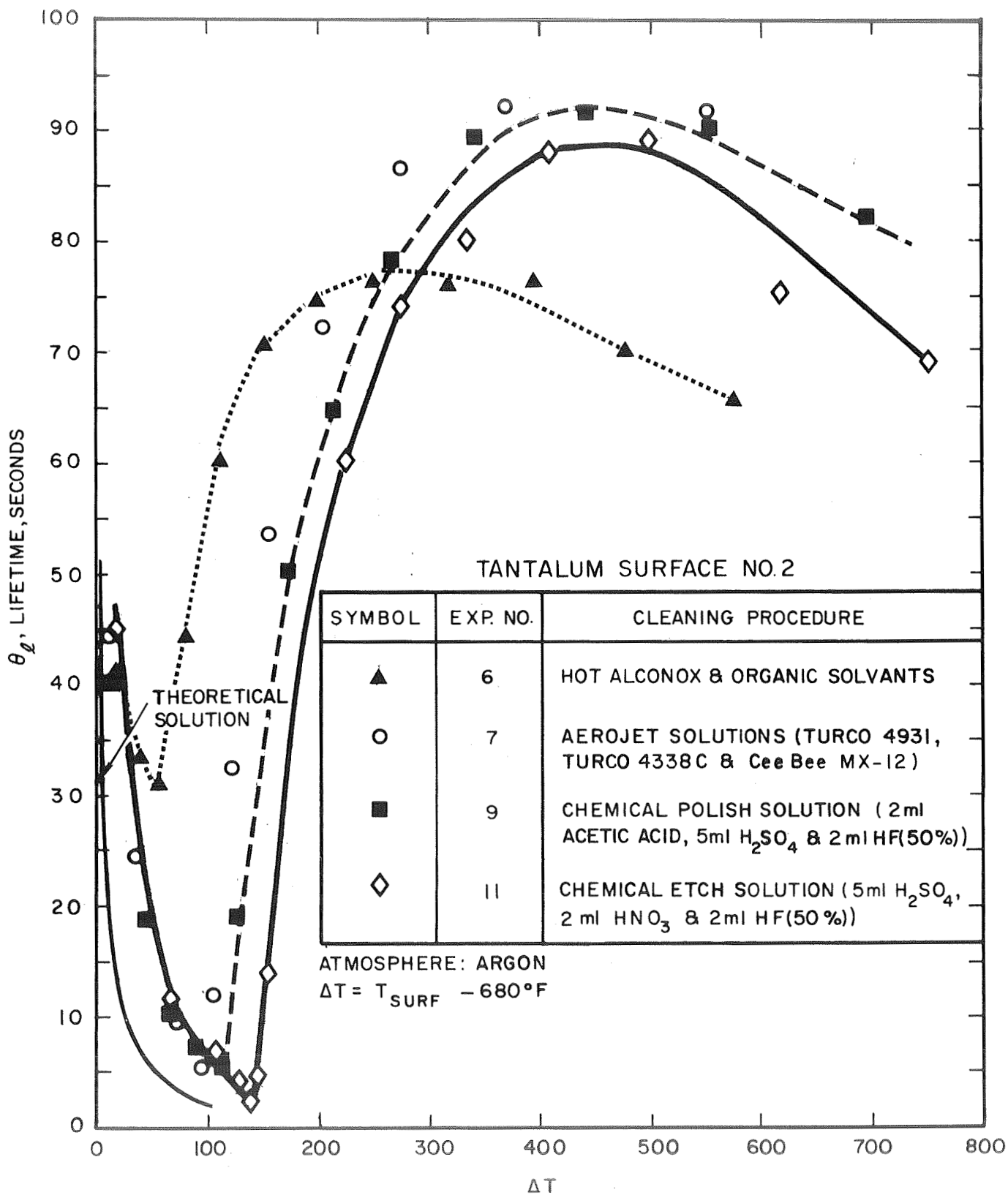
Figure 2. The lifetimes for mercury droplets vaporizing on tantalum surface No. 2.
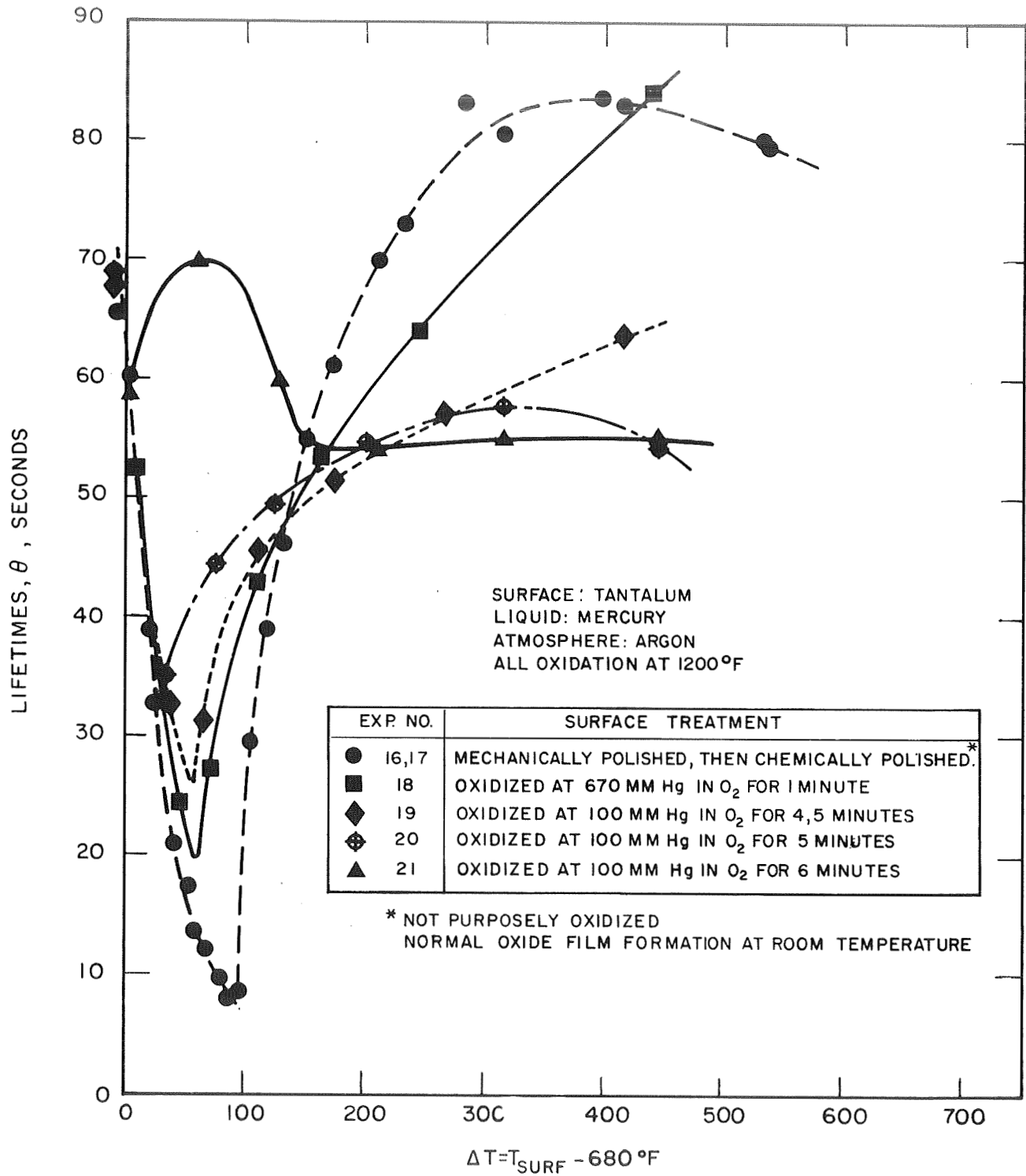
6

Figure 3. The lifetimes of mercury droplets vaporizing on a tantalum surface with various amounts of surface oxidation.
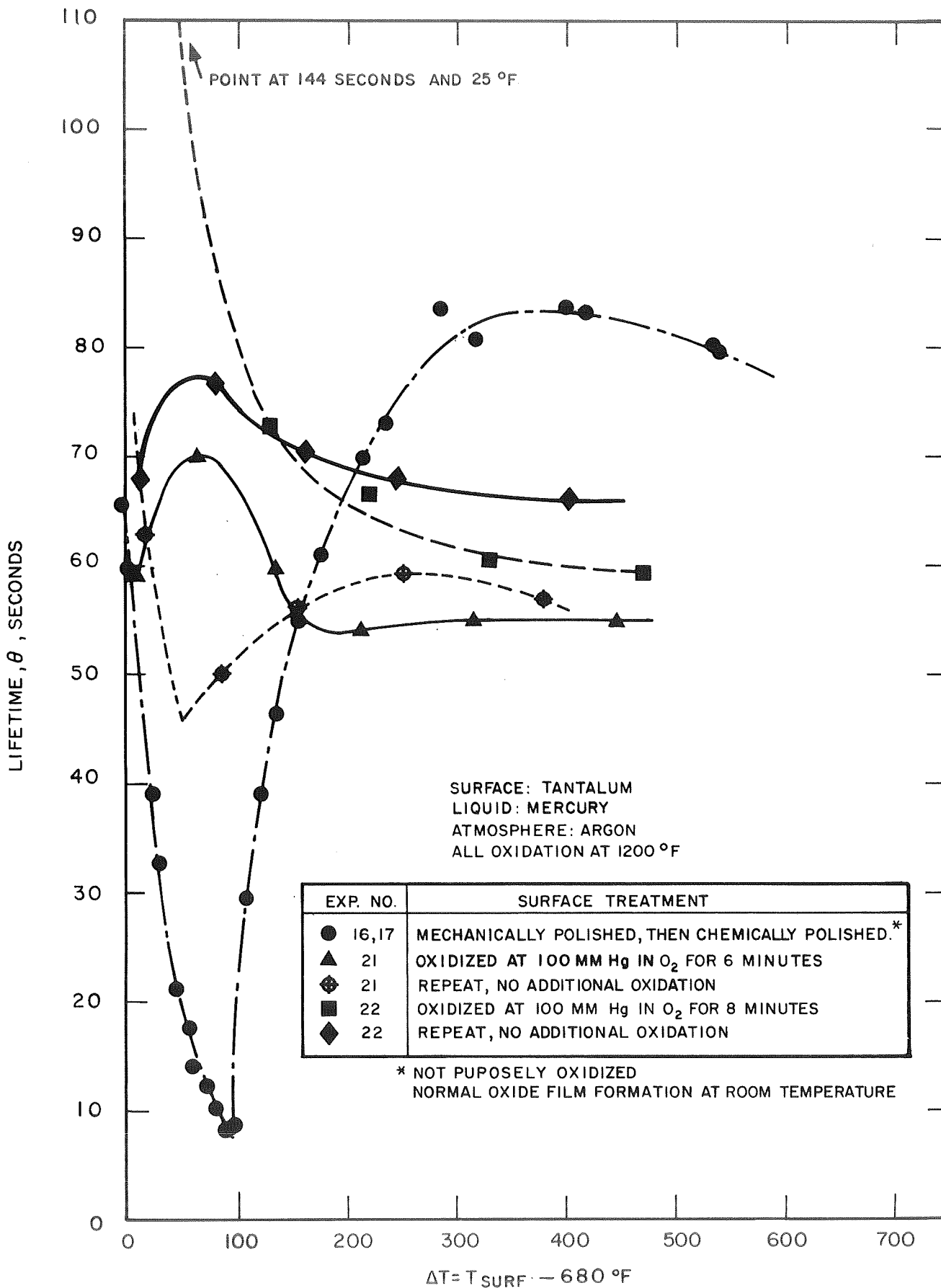
Figure 4. The lifetimes of mercury droplets vaporizing on a tantalum surface with various amounts of surface oxidation. The data presented are a continuation of the data given in Figure 3.

TABLE I

Surface appearance and measured oxide thickness

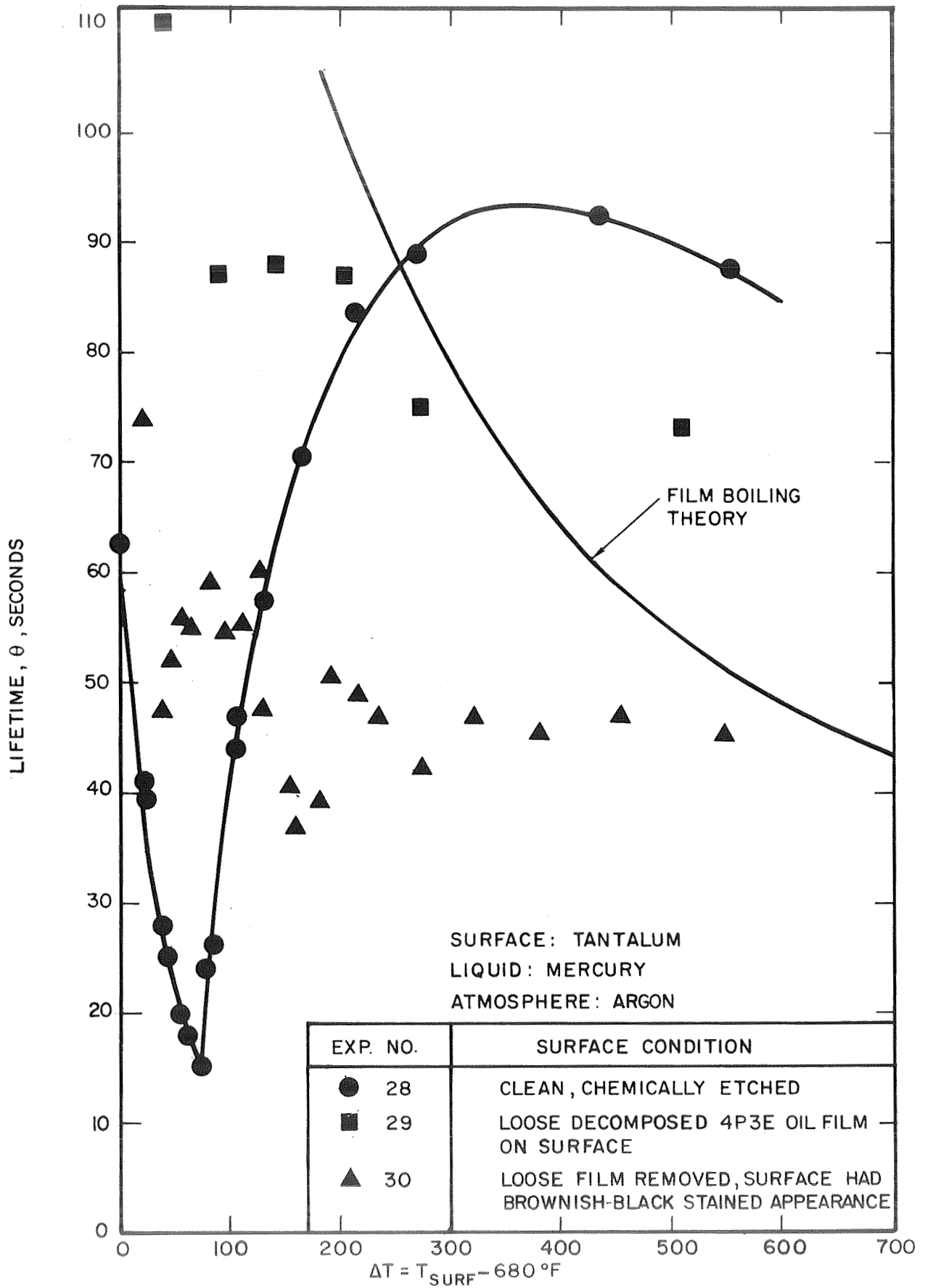| Experiment Number	Oxide Thickness $\times 10^{-3}$ Inches	Physical Appearance of Surface
16	~0	Bright metallic
17	~0	Bright metallic
18	< 0.1	Grey
19	0.2 - 0.5	Darker grey
20	0.4 - 0.7	Grey with few white spots
21	0.4 - 0.9	Grey with increased number of white spots
22	~1 (estimate)	Mostly white adherent crystals with some grey surface

Figure 5. The lifetimes of mercury droplets vaporizing on a tantalum surface with
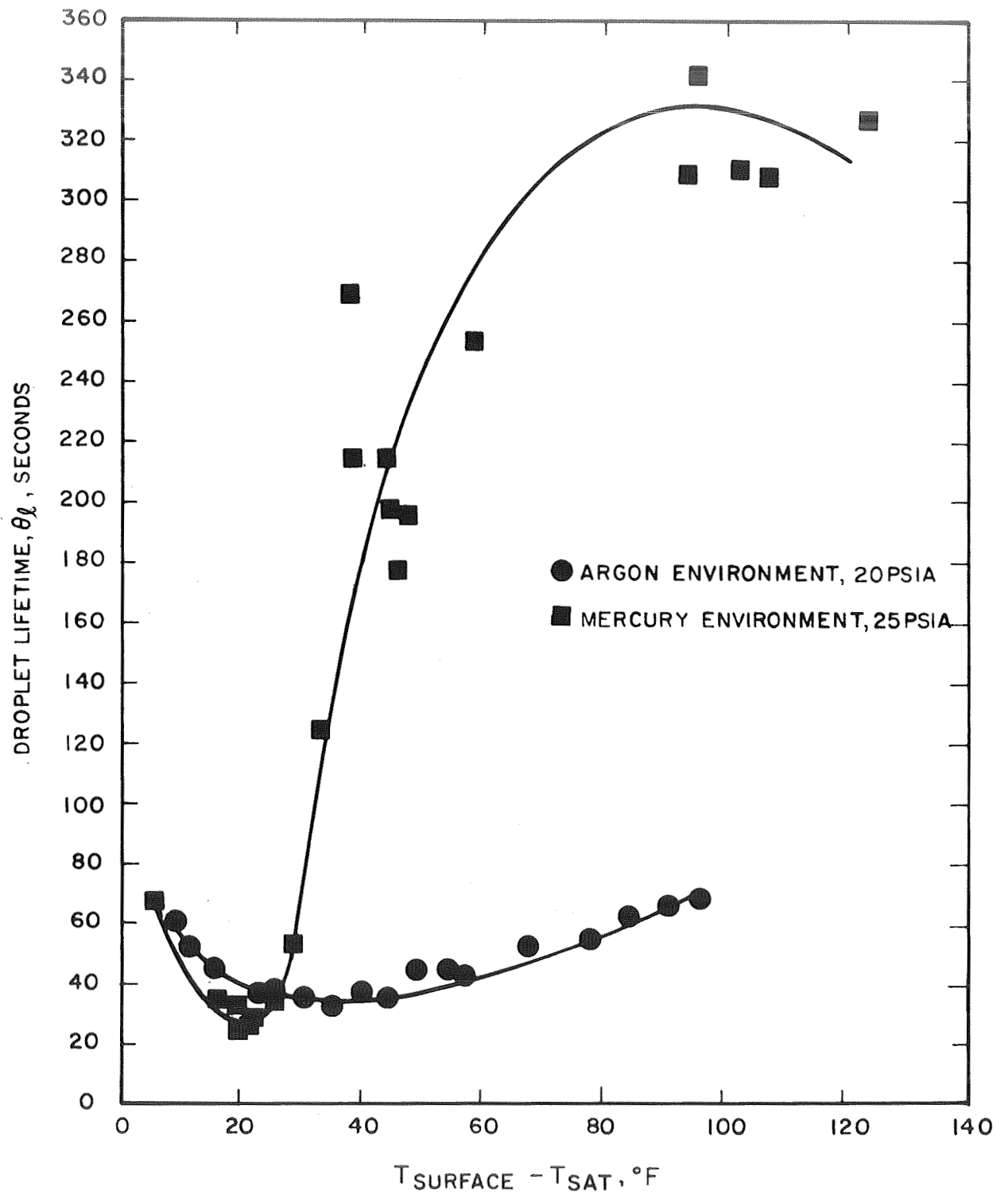various thicknesses of decomposed 4P3E oil deposited upon the surface.

10

Figure 6. The Lifetimes of Mercury Droplets Vaporizing on a
Tantalum Surface in an Argon and Mercury Environment

11

begins to wet clean tantalum at about 900°F; this result was also obtained by the General Electric Company. Geoscience performed additional wetting experiments by introducing argon gas and air; the results showed that in an air environment, significant changes in wetting (contact angle) are in evidence.

In addition to the droplet vaporization and wetting experiments, thermal resistance measurements for decomposed 4P3E decomposed oil deposits were carried out. The measurements were made in a thermal conductivity cell that mainly consisted of a thick copper plate, a layer of decomposed 4P3E oil deposited upon the top surface of the copper plate and a layer of triple-distilled mercury on top of the oil film. The temperature drop across the carbonaceous film was measured when the heat conducted through the cell was at a steady state. The thermal conductivity was calculated from the measured temperature drop and film thickness.

The thermal conductivity for one film was 0.01 Btu/ft hr °F at 105°F. The deposit was one-thousandth of an inch thick and was composed of a soft, granular carbonaceous material. The thermal conductivity for a second film was found to be 0.02 Btu/ft hr °F at 110°F. This deposit was 2.5×10^{-3} inches thick and was also composed of a soft, granular carbonaceous material, but was apparently denser because of the higher deposition temperature involved (1360°F for the second film versus 1260°F for the first film). The density of coke (the carbonaceous residue left when oil is decomposed) is increased with temperature of formation. This may explain why the thermal conductivity of the second film was larger than that of the first film.

Analytical Verification
Analytical studies were conducted in parallel with the experimental work described above. Specifically, the effects of different degrees of wetting, surface roughness and added thermal resistances from contaminant deposits, in addition to droplet vaporization, were considered.

An example of a pertinent droplet vaporization analysis accounts for the effects of the degree of wetting and deposit resistances. A heat rate balance on an idealized, disc-shaped drop is,

$$ q = \frac{t_w - t_s}{\dfrac{\delta_\ell}{k_\ell} \dfrac{1}{A} + \left(\dfrac{\delta_i}{k_i}\right) \dfrac{b_f}{A}} = LG \qquad (1) $$

where

t_w wall temperature

t_s saturation temperature

δ_ℓ thickness for disc-shaped drop

δ_i deposit film thickness on boiler tube surface

12

k_ℓ thermal conductivity of liquid mercury

k_i thermal conductivity of deposit film

L   latent heat of vaporization of mercury

G   rate of mercury vaporization

b_f a shape factor for two-dimensional heat flow through the drop

$$\bar{A} = C \delta_\ell^{\,2}$$

The definition of $\bar{A}$ is based on a postulation that the drop diameter is proportional to the drop disc thickness (the idealized disc-shaped drop retains its shape as evaporation proceeds). The term C is a geometrical factor that relates $\bar{A}$ to δ_ℓ. In the following development, b_f is taken as unity (a first approximation). From Equation (1), there results

$$G = \frac{\left(t_w - t_s\right) C \delta_\ell^{\,2}}{L \left(\dfrac{\delta_\ell}{k_\ell} + \dfrac{\delta_i}{k_i}\right)} \tag{2}$$

The mass flow rate of the vaporizing mercury from the drop, G, is also equal to

$$G = -\frac{d(\text{mass})}{d\theta} = -\frac{d\left(\dfrac{\pi}{4} \delta_\ell^{\,2} \delta_\ell w_d\right)}{d\theta} \tag{3}$$

where

     w_d density of liquid mercury

     θ time

From Equations (2) and (3) there results

$$\frac{-3\pi w_d L}{4 C \left(t_w - t_s\right)} \int_{\delta_{\ell_0}}^{\delta_\ell} \left(\frac{\delta_\ell}{k_\ell} + \frac{\delta_i}{k_i}\right) d\delta_\ell = \theta \tag{4}$$

13

or

$$\frac{3}{8}\frac{\pi}{C}\frac{w_d\, L\, \delta_{\ell_o}^{2}}{k_\ell\left(t_w - t_s\right)}\left[1 - \left(\frac{\delta_\ell}{\delta_{\ell_o}}\right)^{2}\right] + \frac{3\pi\, w_d\, L\, \delta_i}{4Ck_i\left(t_w - t_s\right)}\delta_{\ell_o}\left(1 - \frac{\delta_\ell}{\delta_{\ell_o}}\right) = \theta \qquad (5)$$

When $\delta_\ell = 0$, $\theta = \theta_\ell$ (droplet lifetime), or

$$\theta_\ell = \frac{3\pi\, w_d\, L\, \delta_{\ell_o}^{2}}{8Ck_\ell\left(t_w - t_s\right)}\left[1 + N\right] \qquad (6)$$

where

$$N \equiv \frac{\dfrac{\delta_i}{k_i}}{\dfrac{\delta_{\ell_o}}{2k_\ell}}$$

This lifetime expression is similar to the result obtained for a constant contact area case, except that θ_ℓ for the receding contact area case is greater by $3\pi/4C$. Both solutions have been used to calculate coke film thicknesses by applying the theory to mercury droplet lifetime measurements in the surface vaporization region (taken from Figure 8, page 18, of reference 1). A comparison of the calculated and measured film thicknesses is given in the table below:

Mix 4P3E Coke Thickness in Microinches

(for $C = \dfrac{\pi}{4}$, an approximation)

Experiment Number	Measured Thickness	Computed Thickness (Constant Area Analysis)	Computed Thickness (Receding Area Analysis)
29	300	292	169
30	100	46	28

The experimentally-observed coke thicknesses are of the same order of magnitude as predicted values for the two models; for the specific set of data considered, the constant contact area model appears more applicable. In general, however, it is believed that a receding contact area model may be more appropriate for a surface with a coke deposit.

The influence of the presence of a surface coke deposit in a boiler tube is to reduce the equivalent boiling conductance (for a rotational flow system where a liquid metal annulus exists at the wall*); the defining equation is:

$$U = \frac{1}{\left(\dfrac{\delta}{k}\right)_\ell + \left(\dfrac{\delta}{k}\right)_i} \tag{7}$$

where

$\left(\dfrac{\delta}{k}\right)_\ell$ ratio of liquid metal thickness to thermal conductivity

$\left(\dfrac{\delta}{k}\right)_i$ ratio of surface coke deposit thickness to thermal conductivity

Typical reductions in heat transfer for this mechanism were described analytically and experimentally[1]. From the past research, the thermal conductivity of decomposed 4P3E oil films was determined to fall in the range 0.01 to 0.02 Btu/hr ft °F. The thickness of the coke layer can be estimated from the oil deposition research discussed in the next paragraph.

---

*If rotational flow does not exist or if it is not strong, the liquid annulus can be ruptured as a result of poor wetting at the coke deposit thereby reducing heat transfer still further.

C. 4P3E Oil Transportation, Decomposition and Deposition

On the basis of the droplet vaporization studies with contaminated heat transfer surfaces (as well as past experience with forced convection liquid metal boiling), it was felt at the beginning of these studies that 4P3E oil transportation, decomposition and deposition in SNAP-8 boiler tubes could significantly change the heat transfer and pressure drop performance; the conditions under which this could occur were next studied analytically and experimentally.

Analytical Transport Studies

Oil transport in system piping leading to the boiler was postulated to consist of viscous annular oil film flow at the duct walls (the oil being moved by turbulent liquid mercury flow shear and the pressure gradient). The oil source can be either continuous or a sudden discharge at the pump seal. An analytical expression for the oil film velocity was primarily based on a previous analysis made by Geoscience[3] which described this type of two-component flow momentum transfer in a circular tube; the solution for this model (viscous annulus with a turbulent core) was found to be:

$$\frac{8\pi}{\zeta} \left(\frac{g r_0 \mu_1}{G_1} \right) \frac{\rho^5}{X} - \frac{\rho^4}{4} + \frac{\rho^2}{2} - \frac{1}{4} = 0 \qquad (8)$$

and

$$\frac{\left(\dfrac{\partial p}{\partial x} \right)_{two\ comp}}{\left(\dfrac{\partial p}{\partial x} \right)_{core\ fluid\ alone}} = \frac{\dfrac{\zeta}{\zeta_p}}{\rho^5} \qquad (9)$$

where

$$X = \frac{G_1 \mu_1 w_0}{G_0 \mu_0 w_1}$$

$$\rho = \frac{r_1}{r_0}$$

16

ζ Weisbach friction factor at the annulus-core interface (oil-mercury boundary)

ζ_p Weisbach friction factor for tube wall

r_0 tube inside radius

r_1 radius to annulus-core interface (oil-mercury boundary)

μ_0 viscosity of annulus fluid (oil)

μ_1 viscosity of core fluid (mercury)

G_0 flow rate of annulus fluid (oil)

G_1 flow rate of core fluid (mercury)

w_0 density of annulus fluid (oil)

w_1 density of core fluid (mercury)

$\dfrac{\partial p}{\partial x}$ axial pressure gradient

The mean velocity of an annular oil film, $\bar{u}$, can be defined as,

$$\bar{u} = \frac{G_0}{w_0 \, 2\pi \, r_0 \, \delta} \qquad (10)$$

where the annular area is $2\pi r_0 \delta$, and δ is of oil film thickness.

If the wall is not completely covered by the oil film (for the same film thickness), then the actual oil flow rate would be reduced by a factor, f, which, in essence, represents the fraction of the covered or wetted circumference, namely,

$$f \equiv \frac{G_{0_f}}{G_0}$$

The oil film thickness, δ, can be expressed as

$$\delta = (r_0 - r_1) \frac{r_0}{r_0} = r_0 (1 - \rho) \tag{11}$$

Upon substituting Equations (10) and (11) into the inverse of the flow function X, one obtains,

$$\frac{1}{X} = \frac{2 \pi r_0^2 \mu_0 w_1}{G_1 \mu_1} (1 - \rho) \bar{u} \tag{12}$$

Upon substituting Equation (12) into Equation (8), there results

$$\left(\frac{8 \pi}{\zeta}\right)\left(\frac{gr_0}{G_1}\right) \frac{2 \pi r_0^2 \mu_0 w_1 \bar{u}}{G_1} (1 - \rho) \rho^5 = \frac{\rho^4}{4} - \frac{\rho^2}{2} + \frac{1}{4}$$

or

$$\bar{u} = \frac{f_5(\rho)}{\left(\frac{16 \pi^2}{\zeta}\right)\left(\frac{r_0^3}{G_1^2} g \mu_0 w_1\right)} \tag{13}$$

where

$$f_5(\rho) = \frac{\dfrac{\rho^4}{4} - \dfrac{\rho^2}{2} + \dfrac{1}{4}}{\rho^5 (1 - \rho)} \tag{14}$$

18

It is postulated that a given volume of oil, V_O, added to the system (sudden discharge) is evenly distributed along the length of the tube, i.e., at any given instant, δ is constant over the entire length, z (see Figure 7). The oil volume (accounting for partial wall coverage) is then,

$$V_o \equiv 2\pi r_0 f \delta z \tag{15}$$

The variable δ can be expressed in terms of ρ as follows:

$$\rho = 1 - \frac{\delta}{r_0}$$

$$= 1 - \frac{V_o}{2\pi r_0^2 f z} \tag{16}$$

In order to predict oil film velocities from this model for a sudden oil discharge, the following steps are suggested:

1) Calculate ρ from Equation (16) for a given V_O, f, and z.
2) Evaluate $f_5(\rho)$ from Equation (14).
3) Calculate $\bar{u}$ from Equation (13) for the particular values of r_0, μ_0, w_1, G_1, and ζ. The friction factor, ζ, is a complicated quantity that can vary from the smooth pipe Blausius value to rough-wall quantities depending upon the wave characteristics at the interface of the two fluids.

Experimental Transport Studies

An apparatus that made it possible to add 4P3E oil to turbulently-flowing mercury was used to study several different oil transport mechanisms of interest in the SNAP-8 system (see Figure 8). The liquid mercury flow Reynolds numbers attainable in the system were as high as 75,000 which was less than the PCSG design value of 186,000. Mercury temperatures ranged from room temperature to 165°F.

One set of experiments consisted of adding small amounts of 4P3E oil to the wall of a glass test section. Known amounts of oil were added to the mercury flow under controlled conditions. Because the injections were not made uniformly around the entire tube periphery, only a portion of the perimeter (1/3 to 1/2) was covered by the oil film in most cases. A nominal mercury flow rate of 4,100 lb/hr was maintained
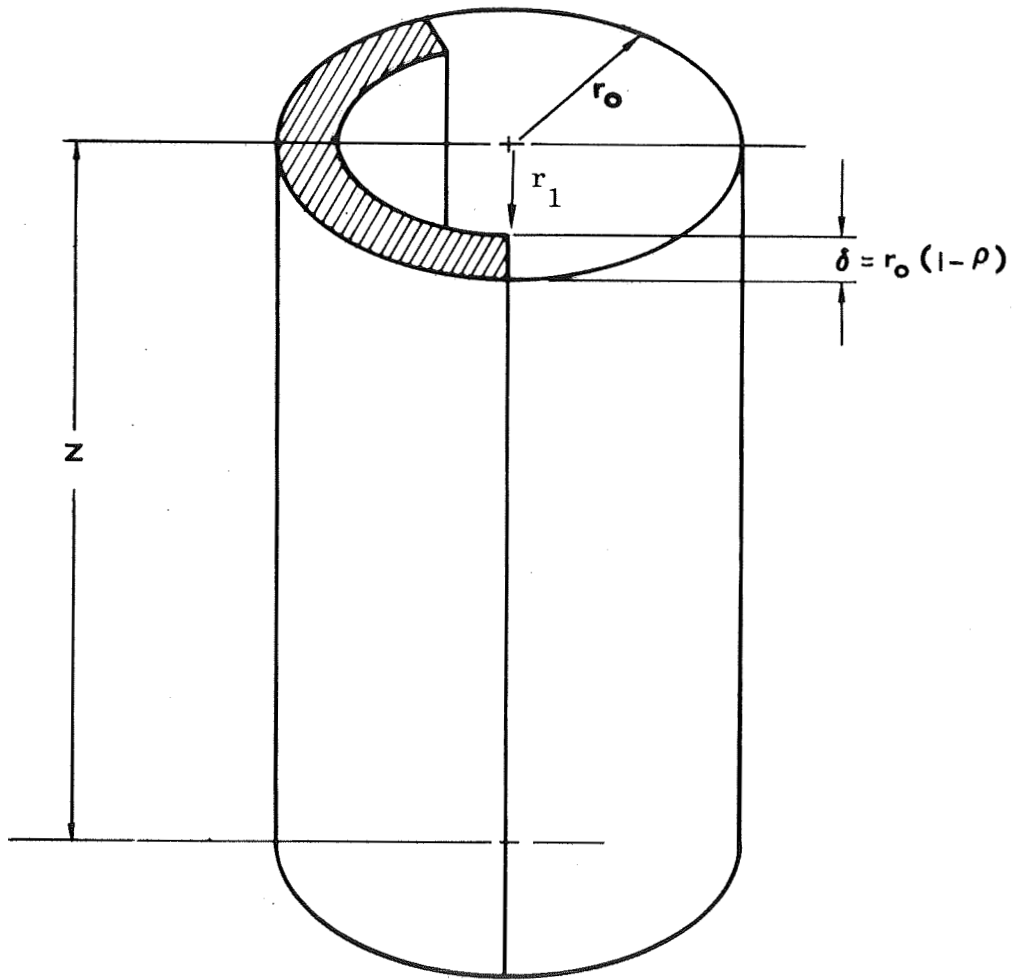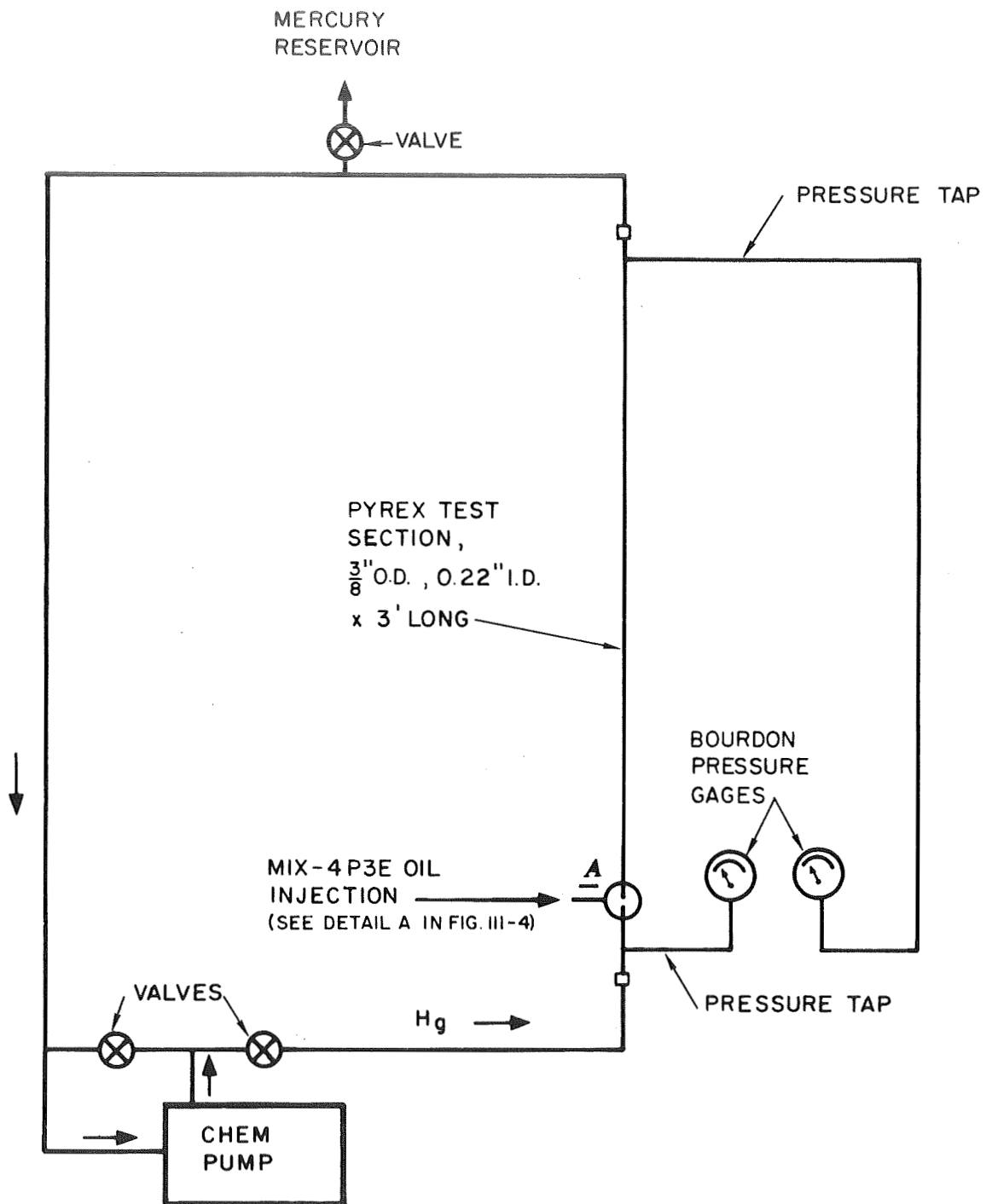
Figure 7. Sketch of oil film geometry.

Figure 8.. Mix-4P3E oil injection apparatus.

during all tests. Usually approximately 0.03 cm^3 of Mix 4P3E oil was injected into the mercury flow in a time period of one to two seconds. This amount of oil was equivalent to the volume estimated by Aerojet staff to leak into the SNAP-8 system in 1000 hours. Upon injection, the oil immediately flowed upward (in the flow direction) along the glass-mercury interface in the form of a film of oil having a curved wave front or leading edge and straight sides. The mean width of the film was approximately half the tube perimeter. There were visible surface waves at the oil-mercury interface and the waves appeared to become less in number and lower when the film moved up the tube and became thinner, as would be expected.

A series of tests were conducted in order to study the behavior of oil transport in mercury when it is introduced into the center of the turbulent mercury core, since it is possible that this could occur in the SNAP-8 system. Using the same test apparatus as reported previously, two methods were used to achieve the test objectives. In one case, oil was introduced at the bottom of the glass tube, at the centerline. In the second instance, oil was injected into the mercury at the pump inlet. Oil injection was achieved by crushing the oil-containing tube flat with a "Visegrip" pliers. Each time the pliers were applied, the 0.060-inch jaws collapsed a corresponding length of tube, resulting in an injection of approximately 0.030 cm^3 of oil. To ensure that the injection tube was properly filled after installation, the tube was carefully squeezed until an oil meniscus appeared at the tip of the tube. After filling the system with mercury, the pump was started and the flow rate adjusted to approximately 4100 lb/hr.

The vertical glass test section was illuminated and three observers were stationed around the column so that the entire periphery could be viewed. The first core injection of 0.03 cm^3 of oil produced no results. Immediately after the second injection, however, fragmented droplets of oil appeared at many locations along the glass wall. The greatest concentration occurred toward the middle and top of the tube. A third injection produced similar results. Strings of tiny oil beads and wavelets were observed in both cases. The oil gradually spread out from these areas until individual spots could no longer be seen. At the end of the experiments, some slight evidence of oil was observed in the sight glass at the top of the tube.

Oil injection at the pump inlet was achieved through a three-foot length of stainless steel tubing inserted through a drilled tee fitting. As in the previous tests, oil injection was accomplished by crushing the injection tube, while the same nominal mercury flow rates were maintained. The glass column and sight glass were cleaned to remove the residue from previous tests. About 30 seconds after the injection of approximately 0.06 cm^3 of oil, it was thought that a few small oil spots appeared on the glass wall. A second injection of approximately 0.09 cm^3 of oil produced even less-pronounced results. A third injection also yielded

inconclusive results. Additional injection tests were performed with the same results.

It was felt that when oil is injected into the pump impeller, the oil is broken into small droplets which impinge upon the system surfaces between the pump and the glass test section.

These studies appear to demonstrate that if liquid oil is introduced into the core of turbulently-flowing liquid mercury, the oil will quickly migrate to the wall in a more-or-less random fashion. Upon reaching the wall, the oil will then spread and distribute itself, eventually covering most, if not all, of the system surface area. If the liquid oil is added to the system at the wall, it will probably never get into the liquid mercury core.

Comparison of Predicted and Experimental Oil Film Transport

In Figures 9, 10, and 11, experimental oil film velocity data are plotted against a background of predicted curves. In order to demonstrate the effect of the three prime parameters, namely oil volume, V_o, temperature, T, and wall coverage factor, f, film front velocity predictions were made for various values for these variables; one parameter was varied in each figure. This approach was used rather than to predict velocities for a specific experimental data set. The difficulty in making such specific predictions was that the prime system parameters were usually not constant throughout a given test. For example, V_O was measured by observing the length of the oil slug in the 1.0 mm diameter orifice in the injection tube. As the oil flowed out of the capillary tube, it entered a bell-shaped divergent section prior to entering the main mercury flow. A portion of the injected oil collected in this region. The actual V_O added to the tube wall could then vary considerably from the intended amount, depending on the superimposed fluid flow oscillations. The second parameter, temperature, was measured precisely at the wall of the steel tubing. In all tests, it was assumed that the injected oil immediately attained the temperature of the flowing mercury. However, it takes time for the temperature equilibration to occur, resulting in significant viscosity changes. This effect was clear when reviewing the velocity vs. distance data at elevated temperatures. The wall coverage factor, f, was also difficult to determine accurately. Often it appeared to be one-half or less, but the interface between the film edge and the wall was not well-defined, especially at greater column heights and higher temperatures. The film front itself was somewhat less obscure because it was slightly thicker and, therefore, more visible. Because of the inconstancies of the major variables during the experiments, representative limiting values of the parameters were chosen for use in the analytical film velocity predictions. Figure 9 shows the effect of varying V_O from 0.003 cm^3 to 0.060 cm^3, at T = 165°F and f = 1. There is a difference of a factor of approximately 15
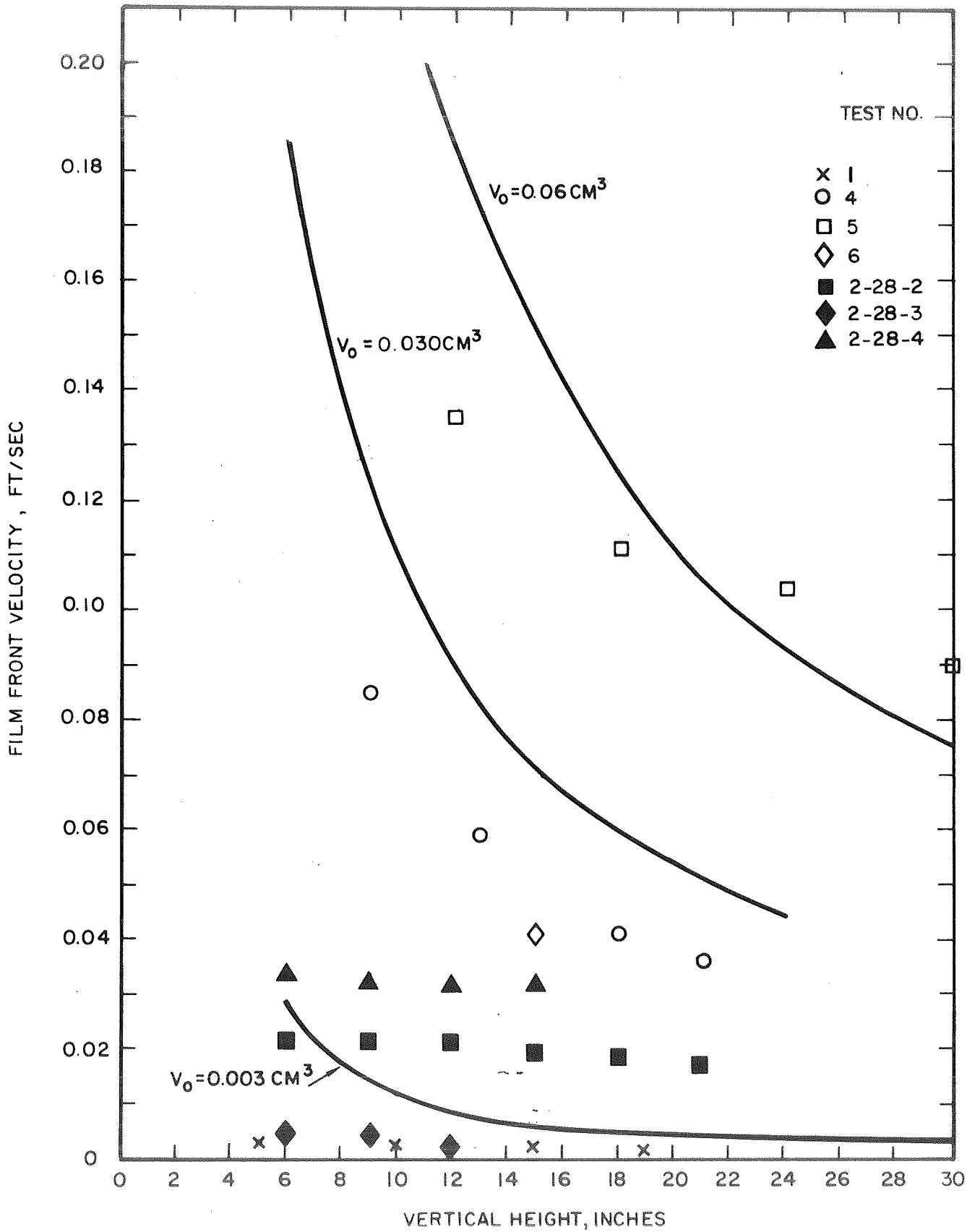
Figure 9. Film front velocity versus vertical height, showing effect of V_o; T = 165°F, f = 1.

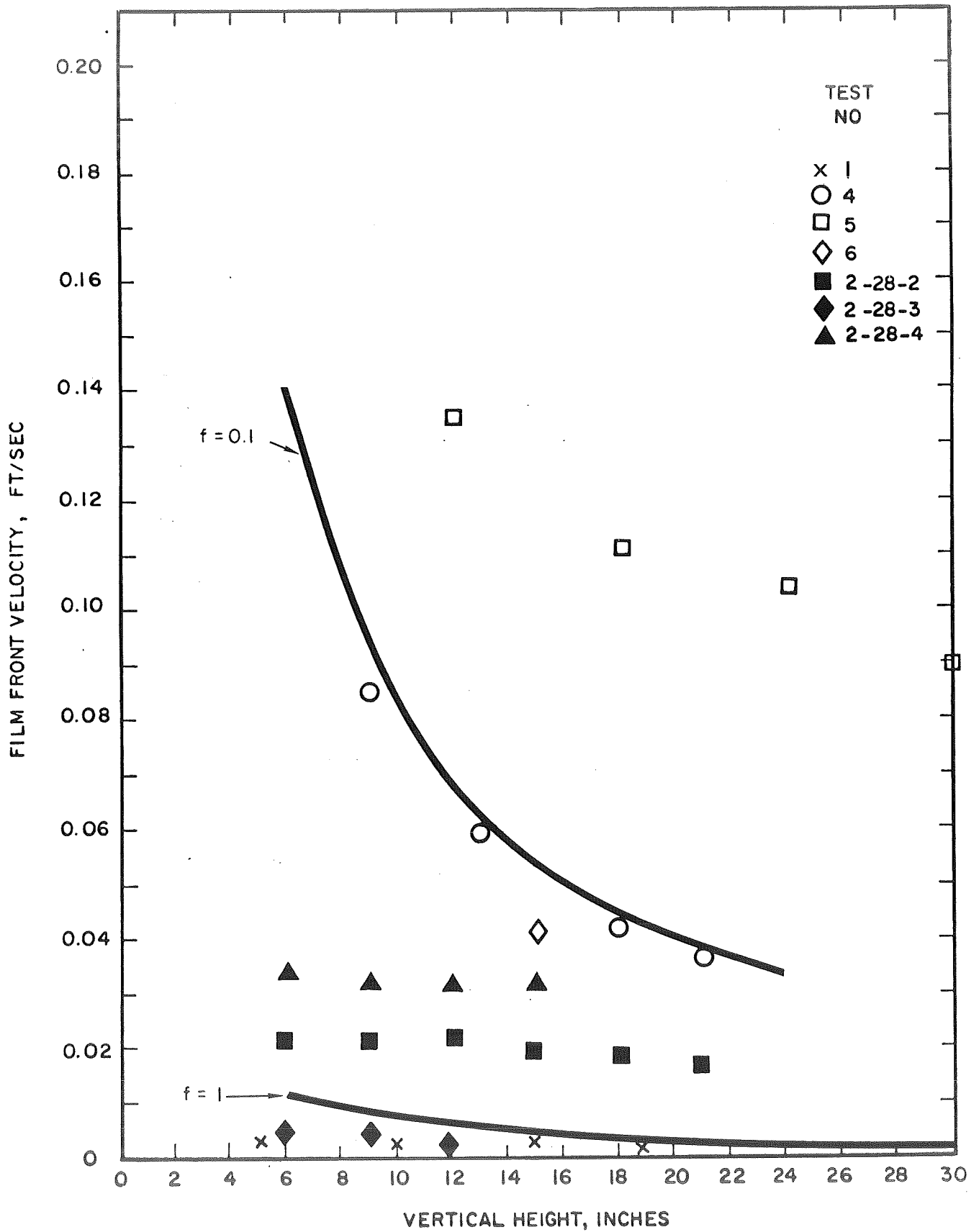Figure 10. Film front velocity versus vertical height, showing effect of f
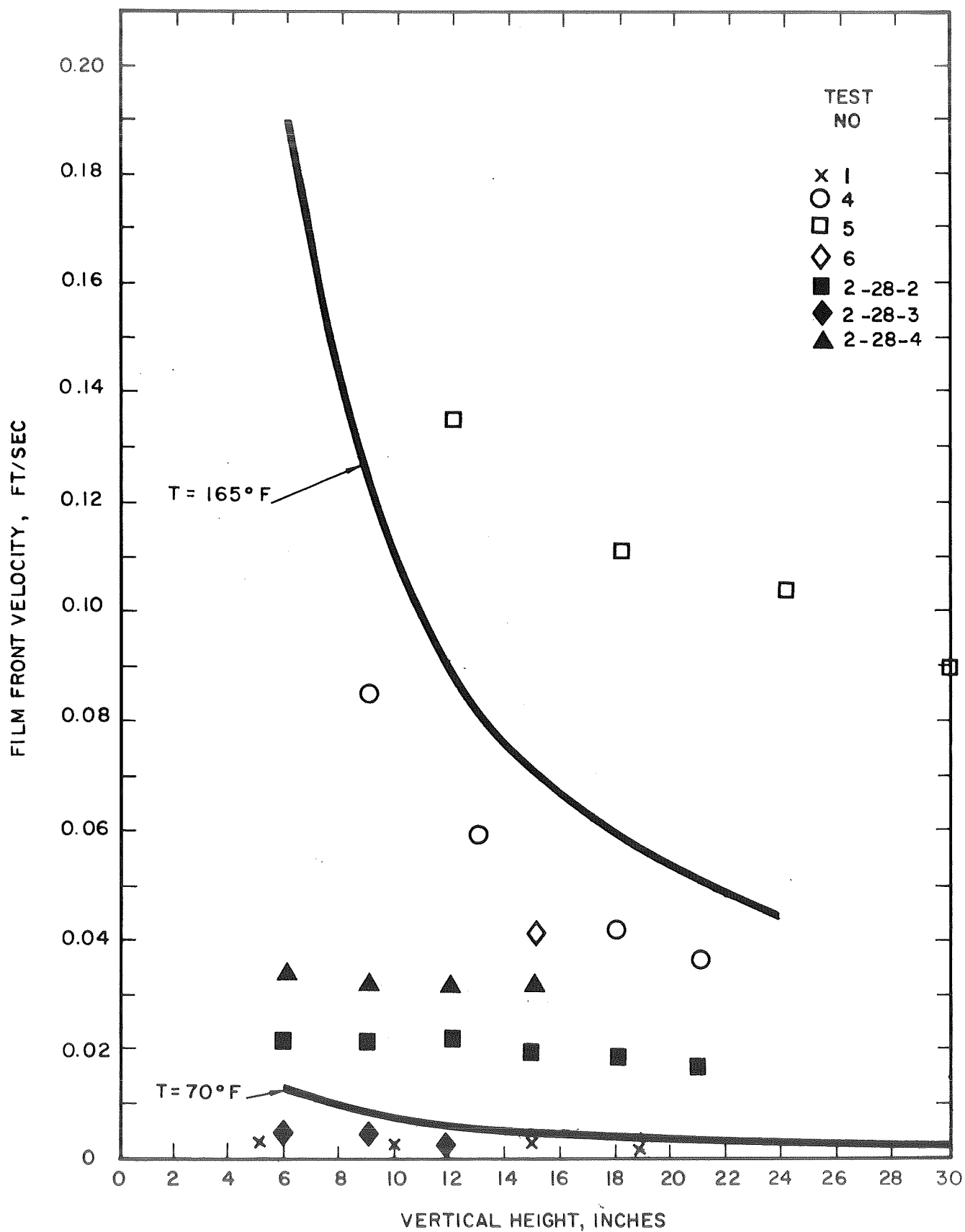factor; V_O = 0.03 cm^3, T = 70°F.

25

Figure 11. Film front velocity versus vertical height, showing effect of temperature; $V_O = 0.03$ cm^3, $f = 1$.

between these extremes. Figure 10 shows the effect of the f function; note the velocity increases about a factor of 10 as f varies from 1 to 0.1; physically, this figure means that for a fixed volume of oil added, a narrower but thicker oil film flows faster than a wider and thinner one. Figure 11 shows that the temperature (or viscosity) is a very important parameter. (The viscosity of 4P3E oil decreases by a factor of six over the temperature range of 70 to 165°F.) The experimental oil film velocity data shown in these figures fall primarily within the predicted limits shown. In the light of the aforementioned experimental difficulties, the comparison of predicted and experimental data is thought to be satisfactory.

Experimental Coking Studies

Data on the decomposition and deposition of 4P3E oil films on SNAP-8 boiler tube walls from Aerojet-San Ramon test results were found to be insufficient to make quantitative evaluations. Therefore, a series of experiments were conducted in order to extend the present knowledge of the decomposition and the corresponding deposition mechanisms.

The first experiment was performed to obtain preliminary information on the coking tendency of the oil. A vertical, 15-inch length of 1/4-inch OD 304 stainless steel tube with a "tee" connection at the lower end was placed in an electrical furnace. The open ends of the tee fitting were capped, forming a small oil boiler. The top end of the tube was left open to the atmosphere. Oil was injected into the bottom of the tee fitting with a hypodermic needle. Thermocouples were installed at the bottom of the tee, in the middle and near the top of the heated section of tube. The system was heated for approximately five hours. During this time it is believed that most, although not all, of the air originally in the tube was removed by diffusion. Some refluxing of the oil vapor was expected to provide a flow of oil through the heated length of the tube.

After the test, the tube was sectioned lengthwise and uniform, thin, hard coke deposits and hard, glossy deposits were found. The former deposit was thought to be deposited from the vapor phase and the latter from the liquid phase. It is believed that the hard, glossy layer defined the beginning of coking at a maximum temperature of about 1000°F under the test conditions. The overall uniformity of the deposit suggested that the entire deposition process is temperature controlled, since one would expect a variation of thickness with tube length if the process were diffusion controlled from the gaseous phase.

In a second experiment, 5 cc of oil was boiled in an Erlenmeyer flask for approximately five hours. Again, reflux action and diffusion were expected to remove most of the air. The purpose of the experiment was to 1) observe decomposition behavior as indicated by a change in boiling temperature, and 2) determine the nature of the decomposition products under these conditions. Boiling commenced at about 800°F. The temperature increased steadily with time, reaching a maximum of 884°F when

the test was ended. The oil darkened early in the test, and was almost black when the test was terminated. A light film was deposited on the wall of the flask, but this proved to be soft and easily removed. The dark oil did not separate into liquid decomposition constituents and, upon microscopic examination, did not contain particulate matter.

A third experiment was conducted to determine the effect of a mixed vapor flow on the deposition mechanism. This study gave information on the mechanism of oil vapor diffusion and deposition in the presence of an inert gas-like mercury vapor. Low velocity argon was allowed to flow through a 3/8-inch OD horizontal stainless steel preheating tube, then into a tee fitting. The flow continued through the tee into a 3/8-inch OD x 3-foot long horizontal glass tube. This tube was inside a close fitting, heavy walled copper tube which, in turn, was heated by two 10-inch long cylindrical heaters equally spaced along the tube length. The other leg of the tee was connected to a small boiler where heated oil vapor was produced. A 3/8-inch OD x 10-inch long stainless steel tube connected the boiler to the tee. Most of this tube length was also heated. After the oil reached the boiling temperature, a small argon flow was initiated. Vapor flow ceased flowing from the glass tube when wall temperatures of ~950° were attained. Maximum glass wall exit temperature at the end of the run was estimated at 1250°F. Examination of the glass tube after the test revealed the same kind of thin, hard coke deposit, as evidenced in the previous experiment (but it was not glassy in character). This deposit also did not appear to be a function of tube length, which suggested that the deposition mechanism from a mixed vapor was also not controlled by a process of oil vapor diffusion from the main flow but rather by temperature.

Analytical Coke Deposition Studies

Data obtained from catalytic cracking processes in the oil refining industry[4] indicate that coking may be a surface-controlled reaction, which is dependent upon the process of diffusion through the coke layer. If one assumes that the diffusion process and, therefore, the coke formation, is inversely proportional to the thickness of the layer and, further, that the coke density remains constant, the differential equation describing the coking mechanism is

$$\frac{dt}{d\theta} = \frac{K}{t} \tag{17}$$

whose solution is

$$t = A \theta^{1/2} \tag{18}$$

where

t, coke layer thickness

θ, time

A, a constant which is a function of both molecular structure of the oil and temperature.

There is an alternate way in which the coking mechanism can be represented. Consider the function,

$$\frac{dC}{d\theta} = -KC \tag{19}$$

where

C, concentration of non-decomposed oil

K, a reaction rate constant expressed as a fraction which is temperature dependent.

Application of this equation to existing data on the decomposition of mix 4P3E oil at 900°F[5] yields a good correlation. Extrapolation of these data from 900°F to 1000°F suggests a value of 3.5 for K. This process, however, is based on the assumption that any slight change in chemical composition of the oil constitutes decomposition. In the same reference, only 60% of the decomposition products were considered "heavy ends." At higher temperatures, at least a portion of these products would be converted to a deposit film. Because only a portion of the decomposition products are thus converted, a new constant, K' (which would be less than 3.5), is introduced. This constant defines oil decomposition to a deposit film. An approximate value for K' has been estimated by applying the decomposition equation to the PCS-1 data. It was assumed that 90% of the oil flowing through the boiler plug insert at 1.5 ft/sec was converted to a deposit film before it left the four-foot long plug insert. In order to satisfy the decomposition equation, the K' for the production of the deposit film must be approximately 1, a value less than 3.5 as noted above. The decomposition equation when expressed in terms of a concentration fraction becomes,

$$\frac{dC'}{d\theta} = -K'C' \tag{20}$$

or

$$C' = C'_o e^{-K'\theta} \tag{21}$$

where

C', concentration of non-decomposed oil expressed as a fraction.

The normalized thickness of the deposited coke film for this model would be 1 - C', a function that has a similar shape with respect to time variation as does the first coking mechanism model, Equation (18).

Synthesis of Oil Transport and Coke Deposition
The following postulates defined an elementary boiler tube coking model applicable to the SNAP-8 system: 1) A fixed volume of oil is introduced instantaneously at some point in the system;[*] 2) the oil film and subsequent coke remain in a liquid state at all times;[**] 3) the physical properties of the oil are not affected by decomposition; volume changes and evolved gases are negligible; 4) initiation of the coking process is thermally controlled and begins at some temperature T = $T_{critical}$; 5) once the critical temperature is reached, the oil temperature remains constant; 6) although transverse oil temperature gradients are neglected, the coke forms in the vicinity of the wall; 7) the oil film velocity is described by the previously-developed analytical oil transport model; and 8) the coking mechanism is described by the functions previously outlined.

The calculation procedure is outlined as follows: From the oil transport model presented previously, calculate the oil film thickness and mean oil film front velocity as a function of distance downstream from the injection point. Next, relate oil

---

*The case of constant oil addition with time can be treated in a similar way but is not discussed here.

**Extrapolation of existing vapor pressure data for 4P3E oil suggests that its boiling point at typical SNAP-8 boiler inlet pressures is in the vicinity of 1125°F. Furthermore, decomposition of the oil would tend to increase the boiling temperature. This probable behavior, plus the results of the above oil deposition studies, strongly suggests that much of the coking occurs in the liquid phase.

30

film front distance to the transport time by evaluating the velocity (distance-time derivative) or

$$\int_{z_1}^{z} \frac{dz}{\bar{u}(z)} = \int_{\theta_1}^{\theta} d\theta \tag{22}$$

Then, cross plot the oil film thickness-distance and distance-time curves to obtain the oil film thickness, δ , as a function of time, θ . Finally, use the coking mechanism deposit thickness-function (Equations (18) or (21)) to obtain the t versus θ relation. A graphical representation of the results is shown in Figure 12. Using the foregoing procedures, the rate at which the coke layer forms can be determined as a function of time and the system parameters. Typical oil and coke layer thickness histories for the model are sketched in Figure 13.

D.   Discussion

Two separate sets of data obtained from PCS-1 operation at Aerojet are referenced to support the proposed boiler deconditioning model based on oil transport, decomposition, and deposition. Boiler BRDC No. 2 demonstrated reduced heat transfer performance in the plug insert region (by an order of magnitude) over its operating period of about a year; the change in heat transfer was defined by the axial NaK temperature profile. When the boiler was opened after operation, no evidence of NaK side boiler tube corrosion was found; whereas pump oil in the mercury circuit was identified, thus supplying evidence for the boiler deconditioning process.

During the operation of boiler BRDC No. 4, a very rapid and extensive degradation in heat transfer along the whole boiler length was recorded. The performance change occurred over the period of a few minutes; after continued operation, however, the initial performance was slowly reestablished suggesting that a discrete oil leak had occurred, and that as time went on the thin oil film was scrubbed away by the mercury flow.
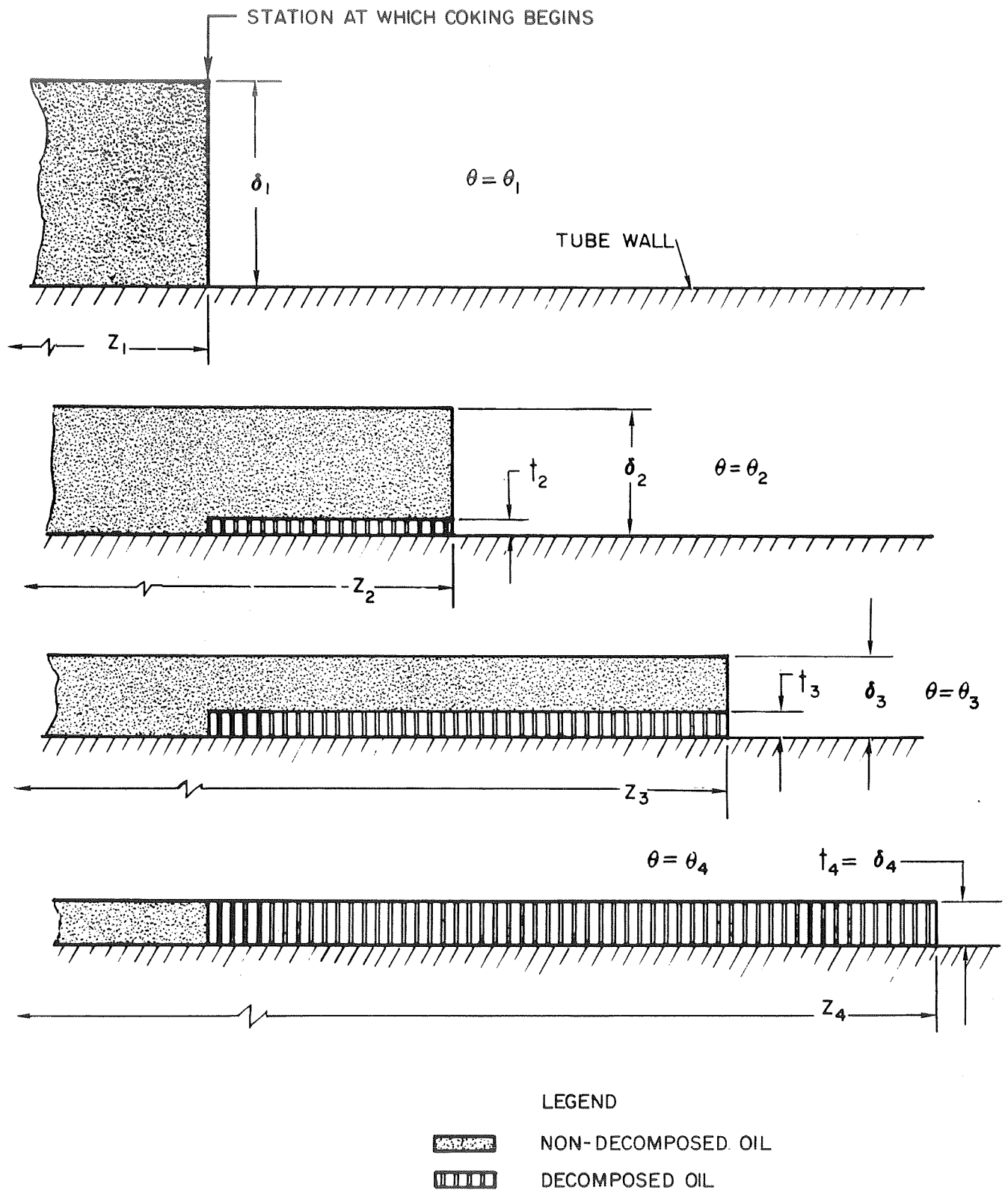
31

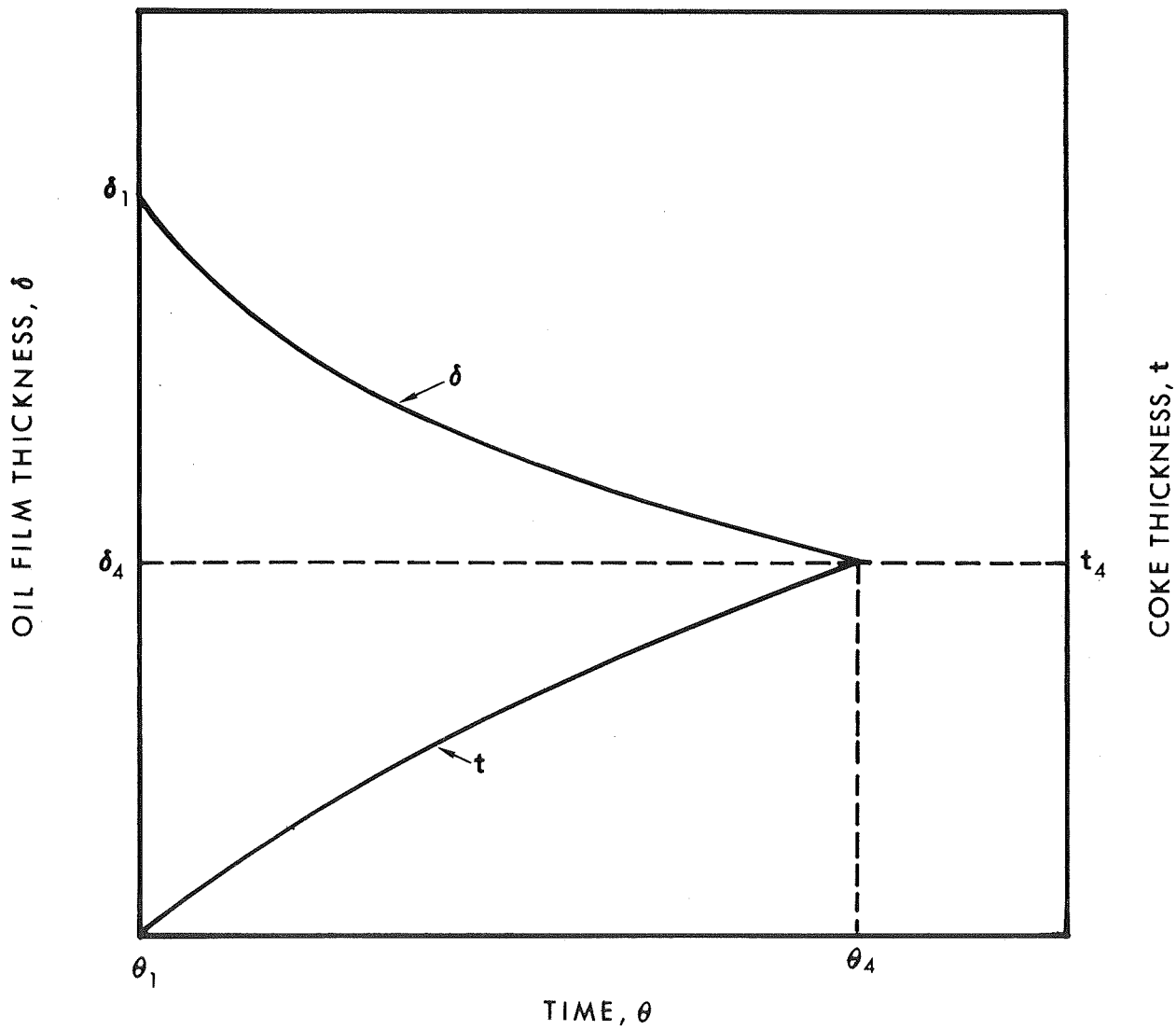Figure 12. Graphical representation of coking in a boiler tube.

Figure 13. Typical oil and coke layer histories in a boiler during the model coking process.

III. TWO PHASE FLOW HEAT AND MOMENTUM
TRANSFER MODELS

A. Definition of Models

A brief review of the more important forced convection boiling flow regimes is given below with corresponding references.

Slug Flow

This flow regime is characterized by alternate slugs of liquid and vapor. It usually occurs for poor wetting liquids under linear flow or helical flow with low rotational flow components. Heat transfer is controlled by convection to the liquid and vapor slugs[3].

Annular Flow

This flow state is defined by a liquid annulus at the boiler wall with a vapor core (the reverse arrangement is also possible under special linear flow conditions). The liquid annulus is normally established because of good liquid wetting at the tube wall or by high velocity rotational flow. Heat transfer is controlled by conduction in the annular film[3].

Wetted-Wall Rivulet Flow

When the liquid annulus in the annular flow state ruptures, rivulets flow down the tube wall. Heat transfer is controlled by vapor convection in the dry areas and liquid conduction in the rivulet areas[6].

Film Boiling Droplet Flow

For non-wetting rotational flow and relatively high wall-saturation temperature differences, film boiling droplets exist contiguous to the boiler wall. Heat transfer is controlled by heat conduction through the vapor film under the droplets and by convection to the vapor flowing adjacent to the droplets[3].

Vapor Flow

In the exit region of a boiler tube where the vapor quality is 100 percent or super heat exists, the classical gaseous forced convection mechanisms are in operation[3].

The differences in heat transfer conductance for these different flow regimes are shown qualitatively in Figure 14.

Separated Flow in a Multi-Slot Insert

Specific heat transfer and pressure drop analyses for the multi-slot insert at the entrance of the Aerojet mercury boiler were conducted. Liquid enters the slotted insert and changes to a two-phase mixture as it passes through this region. Because the slots are machined in a helical fashion on the periphery of the insert rod, it is
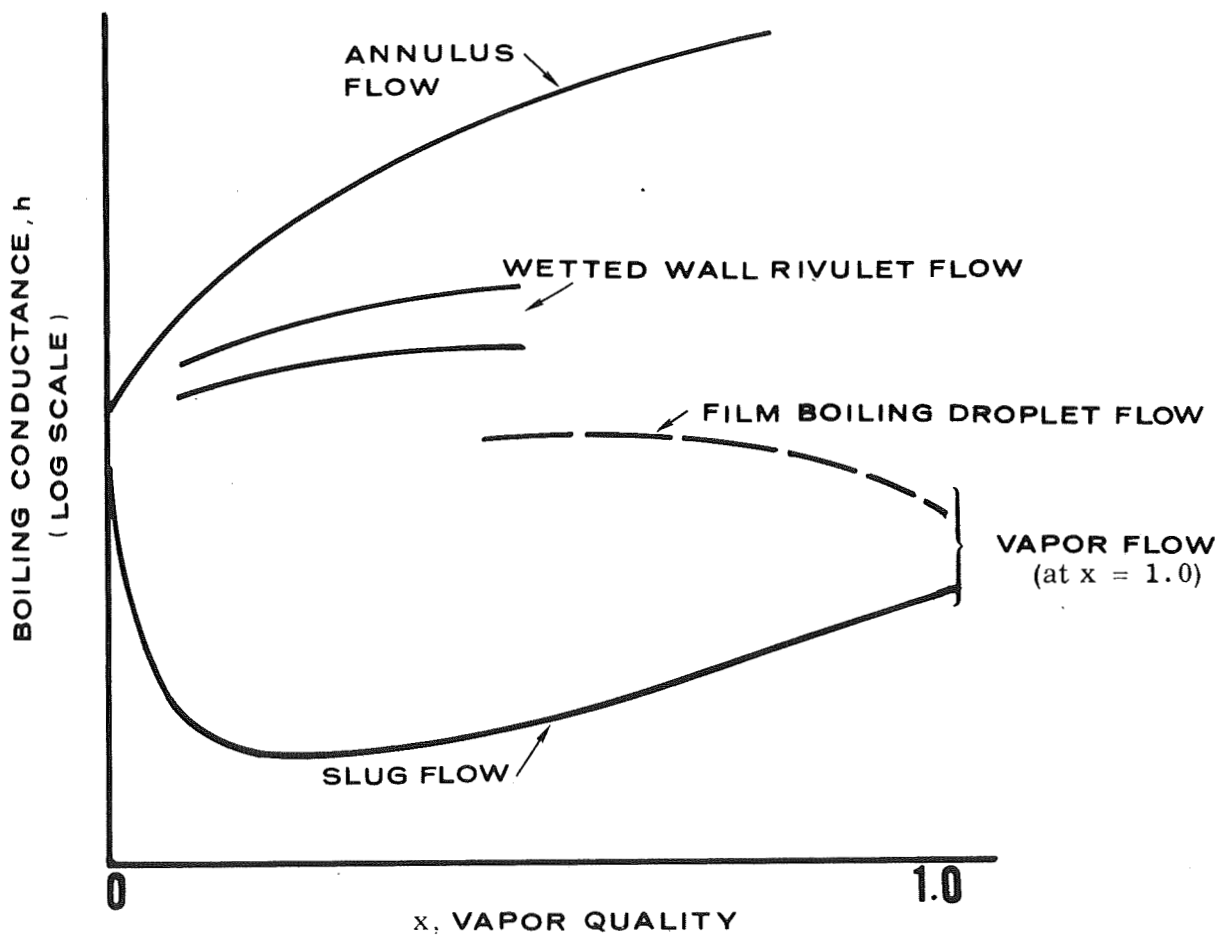
34

Figure 14.

Qualitative representation of forced flow-boiling conductance functions
for several important flow regimes.

believed that the two phases will readily be separated by the centrifugal force field. It is postulated that a thin, liquid layer exists at the outer slot region contiguous to the boiler tube wall and that the remainder of the slot is filled with vapor (see Figure 15).

The pressure drop and heat transfer analyses are shown in some detail in the Appendix (Note 1). The resulting dimensionless liquid-vapor interface radius, ρ, and the two-phase flow pressure drop modulus, $(\partial p/\partial x)/(\partial p/\partial x)_{all\ vap}$ are shown in Figures 16 and 17.

The frictional pressure drop solution can be used to calculate the overall pressure drop across the entrance insert by the use of iterative integral methods. A simplified integral technique for a uniform wall heat flux case is noted in a previous Geoscience report[3] wherein the frictional pressure drop is related to vapor quality. Total pressure losses are obtained by summing the corresponding frictional and momentum change terms.*
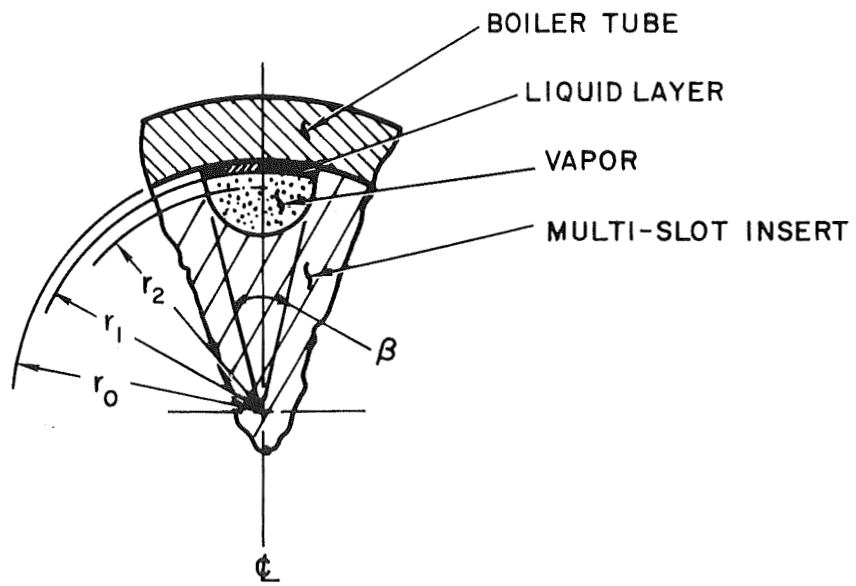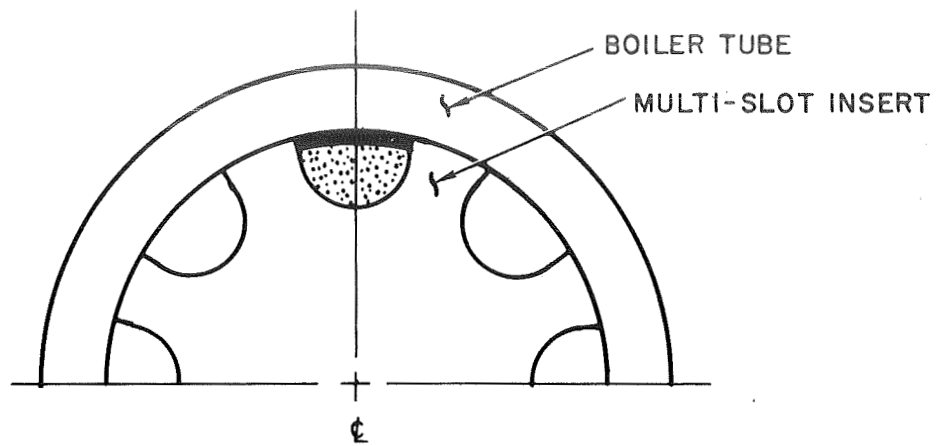
When foreign material such as oxides or oil coke deposits develop at the boiler tube wall, two important consequences result. First, changes in the wetting characteristics can change the phase distribution from liquid annular flow to wetted-wall rivulet flow or even to film boiling droplet flow, thereby changing both the heat transfer and fluid flow characteristics. Secondly, deposition of oil coke deposits add a thermal resistance to the circuit, thereby decreasing the heat transfer.

B.   Applicability Criteria
An important aspect of using boiler design models in heat transfer and pressure drop performance prediction is the determination or specification of what phase distribution or flow regime is in operation. The two most important questions are 1) for the case of helical or linear annular flow under direct contact or surface vaporization, when does rivulet flow start, and 2) is the rivulet flow defined by direct contact (surface vaporization) or by film boiling? These two questions are discussed in the following paragraphs.

---

*A discussion of the important parameter, the friction factor of the vapor-liquid interface, is given in Section C.

BOILER TUBE

MULTI-SLOT INSERT

¢

BOILER TUBE

LIQUID LAYER

VAPOR

MULTI-SLOT INSERT

r_2

r_1

r_0

β

¢

SECTION OF ONE SLOT

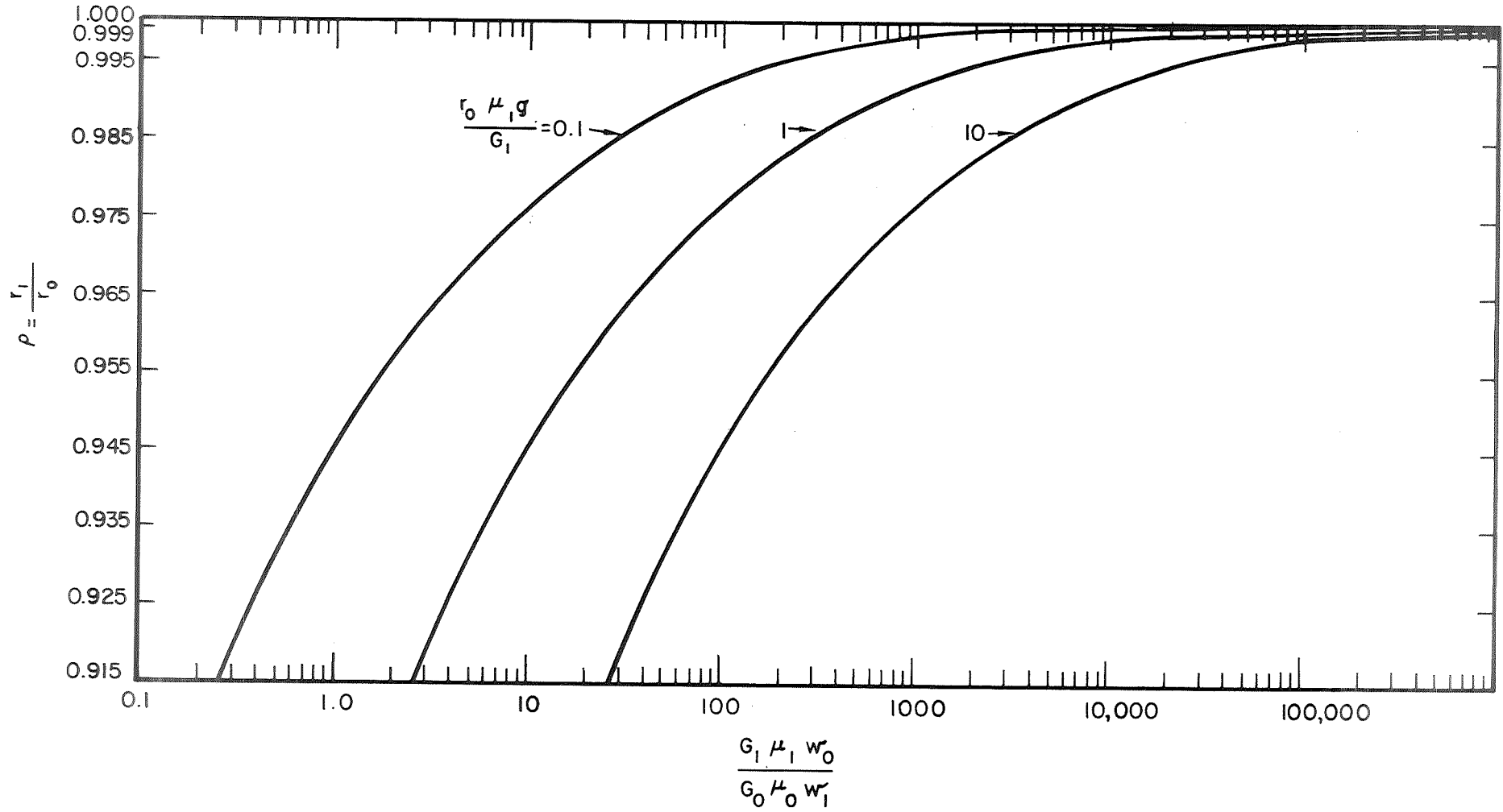Figure 15. Schematic diagram of an idealized multi-slot insert.

Figure 16. Radial liquid-vapor interface ρ for viscous-turbulent two phase flow in the slot with $\zeta = 0.15$, $\zeta_S = 0.03$, $\beta = 0.245$ radians.
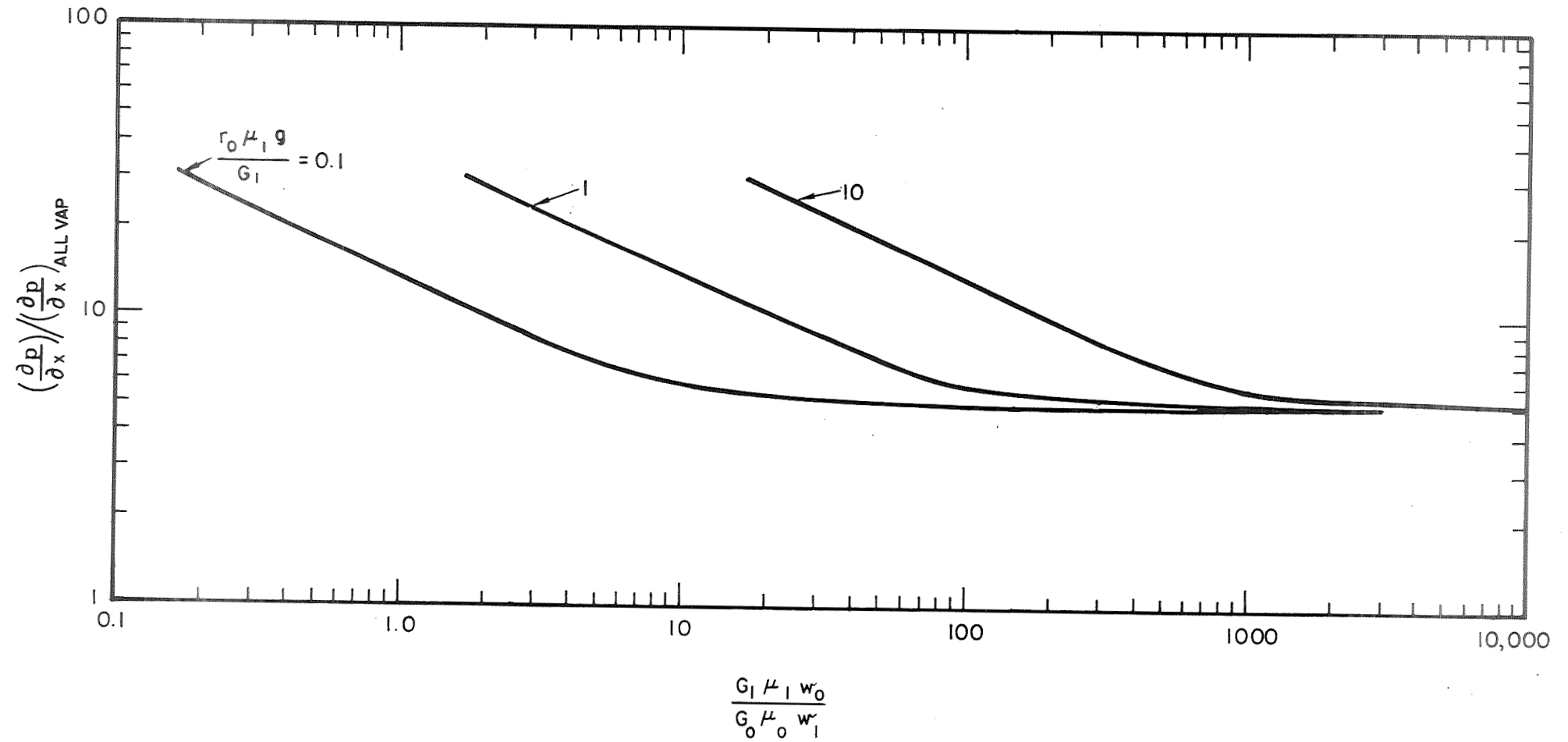
Figure 17. Viscous-turbulent two phase flow pressure drop in the slot with $\zeta=0.15$, $\zeta_s=0.03$, $\beta=0.245$ radians.

Criteria Defining Termination of Annular Flow

Consider a perfectly smooth boiler tube surface upon which a liquid is vaporizing (the liquid is in direct contact with the surface and the boiling consists of surface vaporization or some volume boiling but no film boiling). If the contact angle between the liquid and the wall is zero degrees then, hypothetically, there will be a complete annular liquid film at the wall from vapor qualities ranging from zero to 100 percent. If the contact angle (which is defined by the liquid-vapor, solid-vapor and solid-liquid surface forces) is greater than zero, the width of a liquid rivulet for that particular profile area defined by the contact angle and vapor quality must be compared to the inner circumference of the boiler tube. If the rivulet width is greater than the tube circumference, then the liquid film would not rupture. If the rivulet width is less than the tube circumference, then the liquid film would be separated.

Next, consider a rough boiler tube surface on which a liquid is vaporizing. Several possible processes can occur. If the heights of the surface asperities are greater than the thickness of the liquid film, the contact area of the liquid film will be reduced. If the surface roughness is due to nonhomogeneous structure such as oxide deposits or large metallic grains, changes in local contact angles can also cause local rupture of the liquid film, hence, reducing the contact area. Finally, as a result of surface pits or local areas of non-wetting, film boiling can occur at such points resulting in reduced superheat temperature differences at which surface vaporization ends and transition boiling begins. This change in boiling heat transfer mode is associated with a rupture of the liquid film.

Consider an axial rivulet in a boiler tube. As the contact angle is decreased for a given liquid cross sectional area, the rivulet width increases and finally attains a value equal to the inner perimeter of the boiler tube. At this point the two edges of the rivulet meet and a complete liquid annulus is generated. The particular contact angle under this condition can be called the critical rupture angle (i.e., if the angle is increased slightly, a hydrodynamic or surface disturbance could cause the annular film to rupture). The critical angle can be estimated in the following way. It is postulated that the rivulet profiles are controlled only by surface tension forces (all gravitational forces are presumed to be small). Consequently, the rivulet cross sections are circular in shape. A second approximation involves the cross sectional area of a rivulet. It is postulated that the rivulet cross sectional area is the same as the value for a complete liquid annulus. By equating the width of the rivulet to the boiler tube perimeter and by equating the cross sectional areas of the unruptured annular film to the circular cross sectional rivulet, an equation for the critical contact angle, α_c, can be obtained[6]

in terms of the annulus thickness, δ, and tube radius, r_o.

$$\frac{2\delta}{\pi r_o} (\sin \alpha_c)^2 = (\alpha_c - \frac{1}{2} \sin 2\alpha_c) \tag{23}$$

Next, consider the case where the rivulet contact angle, α, lies in the region $\alpha_c < \alpha$. If, again, it is postulated that the liquid rivulet cross sectional area is equivalent to the cross sectional area for the case of complete wetting (annular liquid film) at a specific vapor quality, equations can be written for the rivulet radius of curvature and for the fraction of the boiler tube area covered by a rivulet, F, on the basis of the geometry involved.

The latter quantity is found to be

$$F = \frac{\sin \alpha}{\pi r_o} \sqrt{\frac{2 \pi r_o \delta}{\alpha - \frac{1}{2} \sin 2\alpha}} \tag{24}$$

for $\alpha_c < \alpha < 90$, and

$$F = \frac{\sin (\pi - \alpha)}{\pi r_o} \sqrt{\frac{2 \pi r_o \delta}{\alpha + \frac{1}{2} \sin (\pi - \alpha)}} \tag{25}$$

for $90 < \alpha < 180°$.

It can be shown that critical contact angles decrease with increasing vapor quality because the annulus thickness δ decreases with vapor quality. Thus, for invariant contact angles, one would expect the annular film to rupture at higher vapor qualities as experimental information indicates. The function F can be shown to decrease with vapor quality and contact angle (above $\alpha = \alpha_c$).

From the discussion presented above, it is clear that it is desirable to have the contact angle be less than the critical rupture angle so that an annular film (and good heat transfer) exists in a boiler. The contact angle of mercury on a clean tantalum surface is a sensitive function of temperature beyond 700°F (see Figure 18). Therefore, surface dewetting and poor heat transfer can result if system temperatures do not fall above this value.
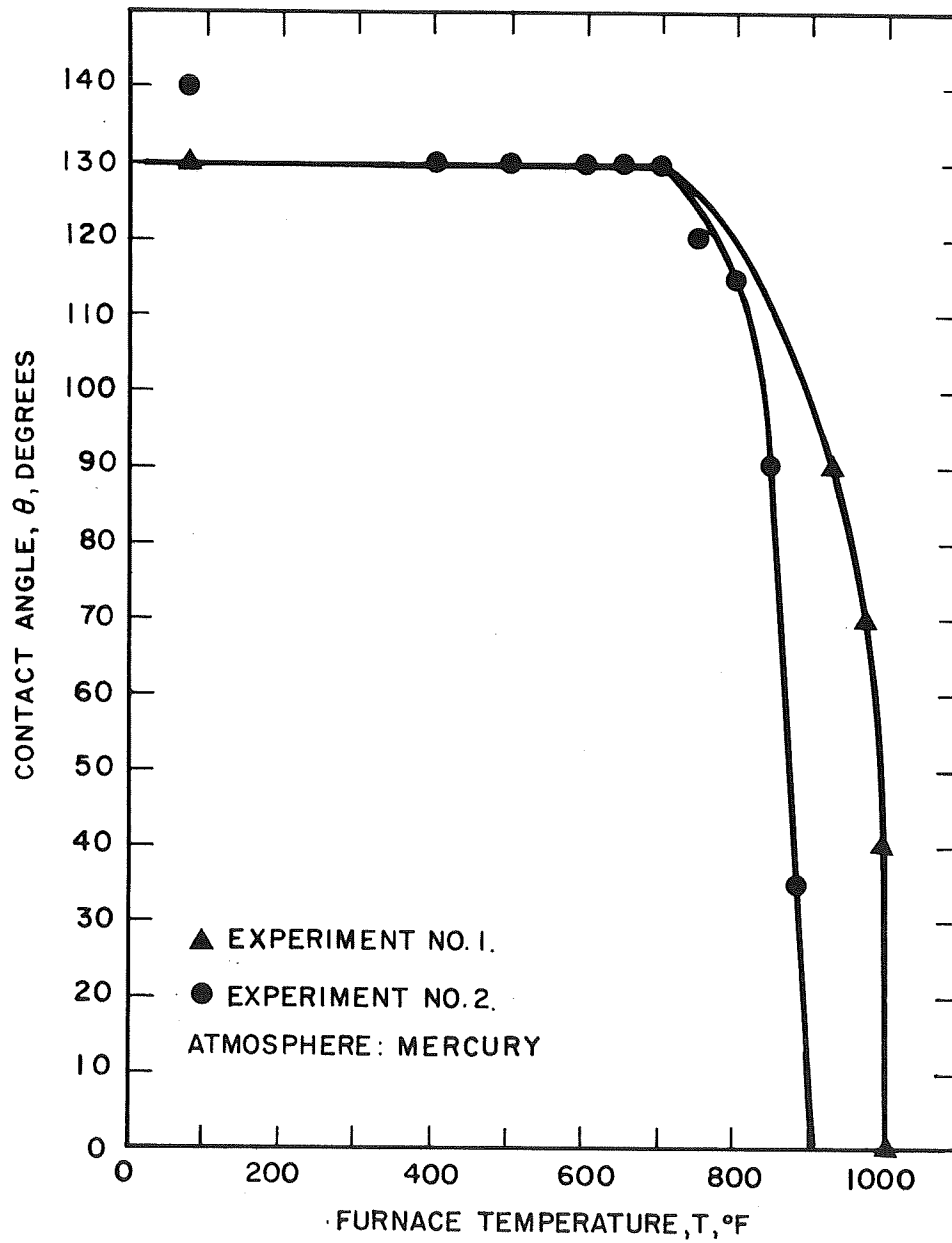
Figure 18. Contact angle formed between a mercury droplet and a chemically etched tantalum surface versus furnace temperature.

Criteria to Distinguish Between Direct-Contact or Film Boiling Rivulet Flow

On the basis of the droplet vaporization studies described previously in this report, direct contact or surface vaporization rivulet boiling in a mercury-tantalum system would terminate in the range $30°F \leq t_{wall} - t_{sat} \leq 100°F$. The film boiling region would begin in the range $250°F \leq t_{wall} - t_{sat} \leq 300°F$. Therefore, it is suggested as a first approximation that 1) the direct-contact or surface vaporization rivulet flow model is used when $t_{wall} - t_{sat} \leq 30°F$, 2) the film boiling rivulet flow model is used when $t_{wall} - t_{sat} > 250°F$, and that a linear proration with Δt is used between these limits (in the transition region). These approximate bounds on the surface vaporization and film boiling droplet flow models are in reasonable agreement with Aerojet evaluations of actual boiler performance results.

C.   Discussion

There are several specific questions relating to boiler design parameters and performance objectives that are considered in the following paragraphs.

Friction Factor Functions for the Liquid-Vapor Interface in a Boiler Tube

An important question arose in connection with Aerojet's pressure drop measurements in the plug insert region of the SB-1 boiler. Specifically, it was found that the experimental friction factors for the liquid-vapor interface in the plug insert (in connection with the annular flow pressure drop model presented in Note 1 of the Appendix) were as much as an order of magnitude greater than smooth wall friction factors and varied with mercury flow rate. The question was, how much greater would one expect them to be? It had been noted in experimental systems at Geoscience for the case of mercury-air flow in glass tubes and the transparent port boiler tube system, that high degrees of surface roughness were in evidence at the interface between the flowing mercury and air or vapor. Therefore, it was thought appropriate to examine available information on liquid mercury surface roughness, friction factors in ducts with rough surfaces, as well as some supporting analytical work.

A series of photographs taken through a transparent port in a boiler tube (mercury boiling with and without helical inserts) can be seen in Figures 19, 20, 21, and 22; these data were obtained from a previous Geoscience phase-distribution study for the AEC[7]. Descriptive notes have been put on the various figures which cover the vapor quality range germane to the SB-1 plug insert. The main purpose for showing these photos is to indicate that even in the case of helical flow, the liquid-vapor interface is not equivalent to that of a smooth pipe. The rivulets and droplets can crudely be approximated by flow over bodies and flow through orifices. One can define the surface roughnesses by obstruction or wave heights, ϵ , (equivalent

All Liquid

Vapor
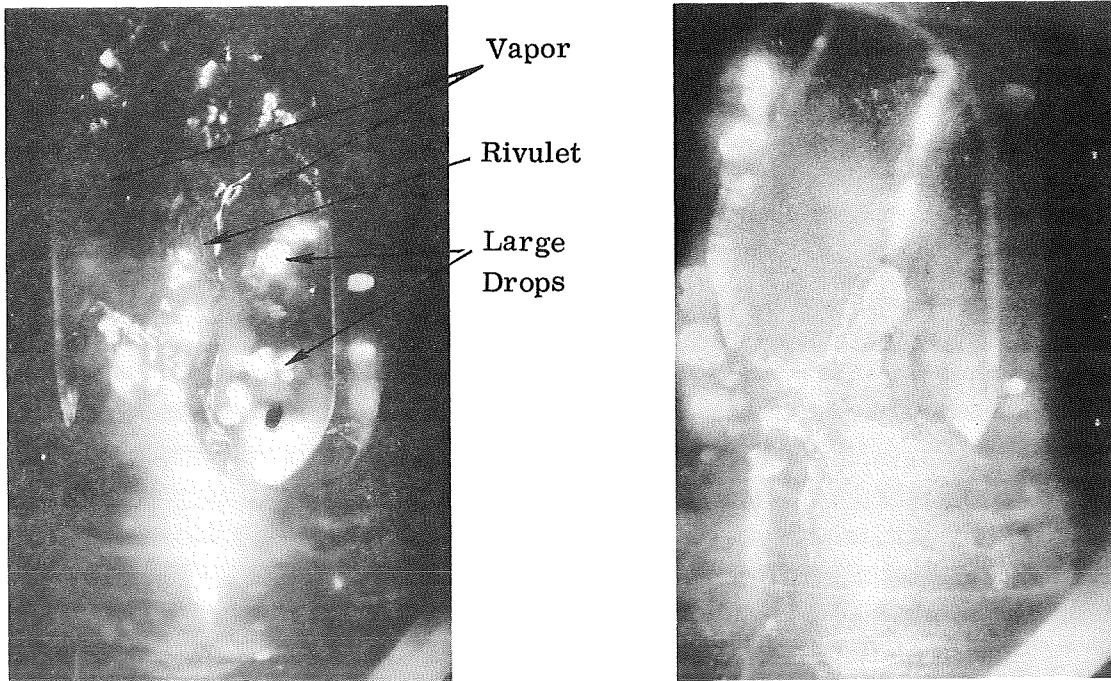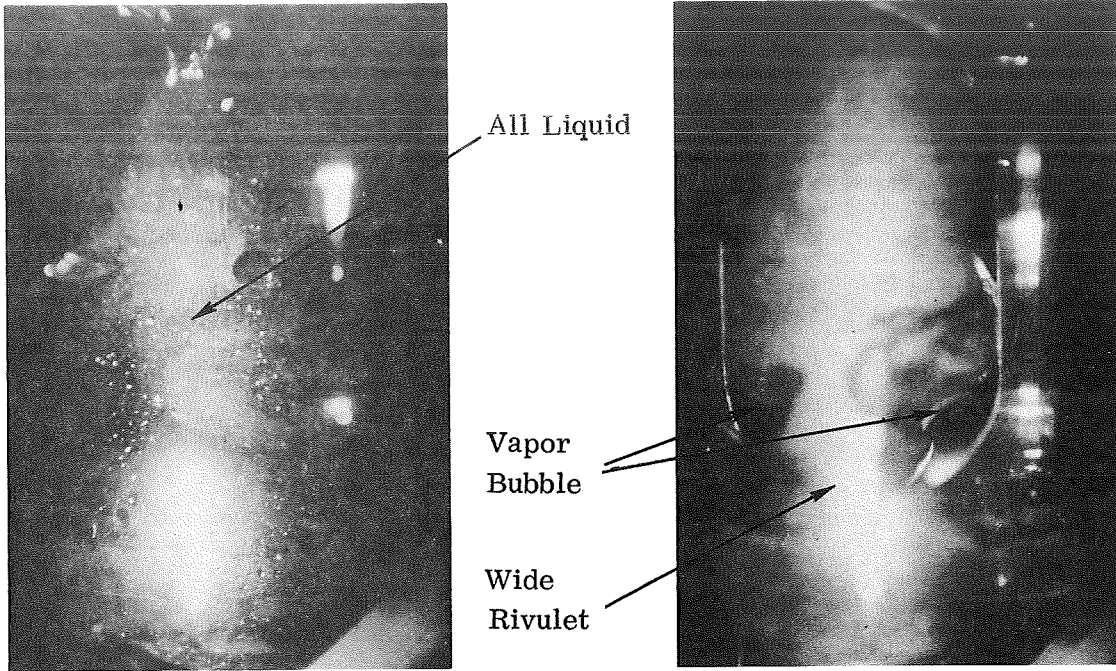Bubble

Wide
Rivulet

Vapor

Rivulet

Large
Drops

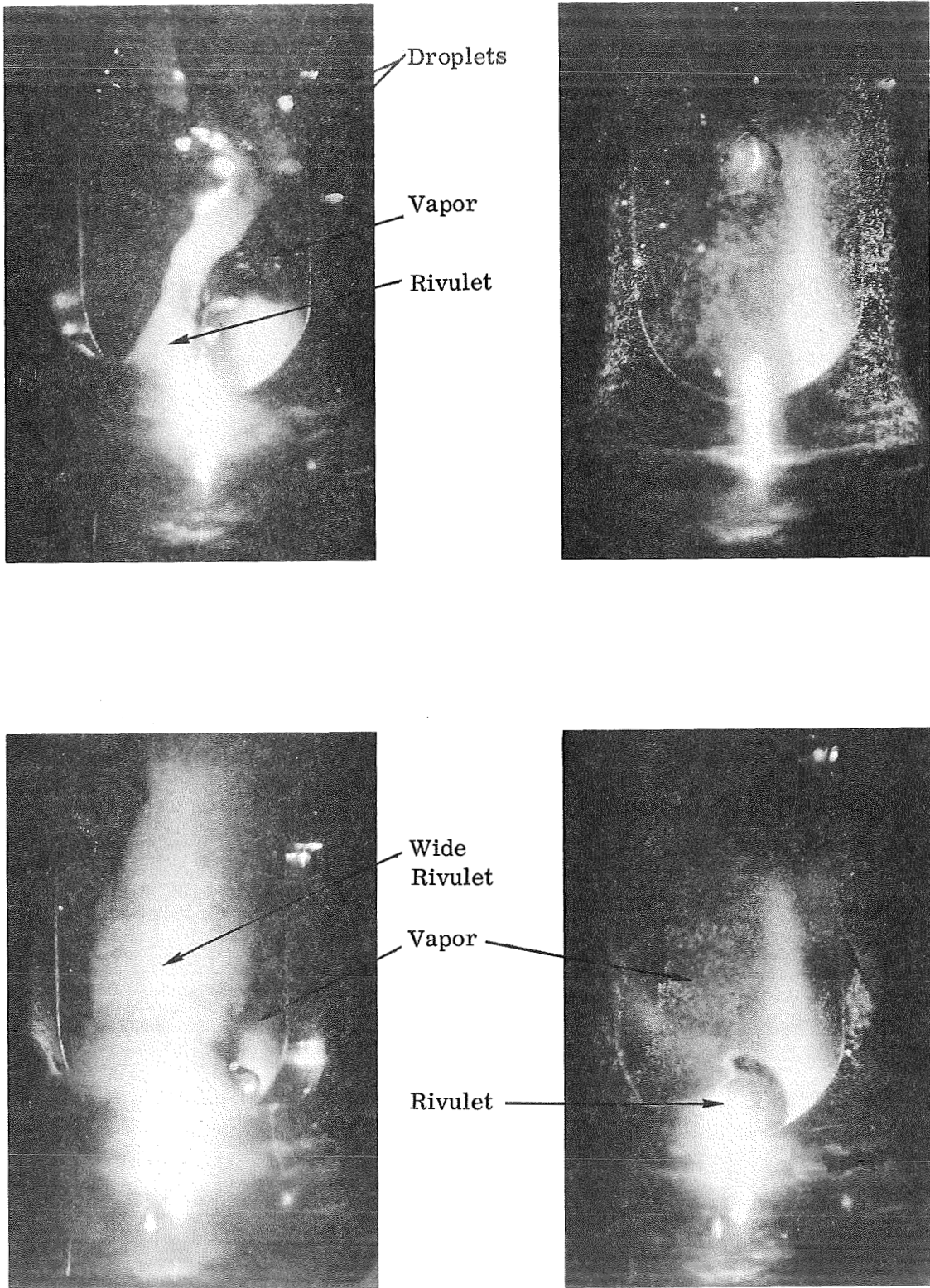Figure 19.   Helical forced flow boiling mercury, 1% vapor quality.

Figure 20.   Helical forced flow boiling mercury, 4% vapor quality.
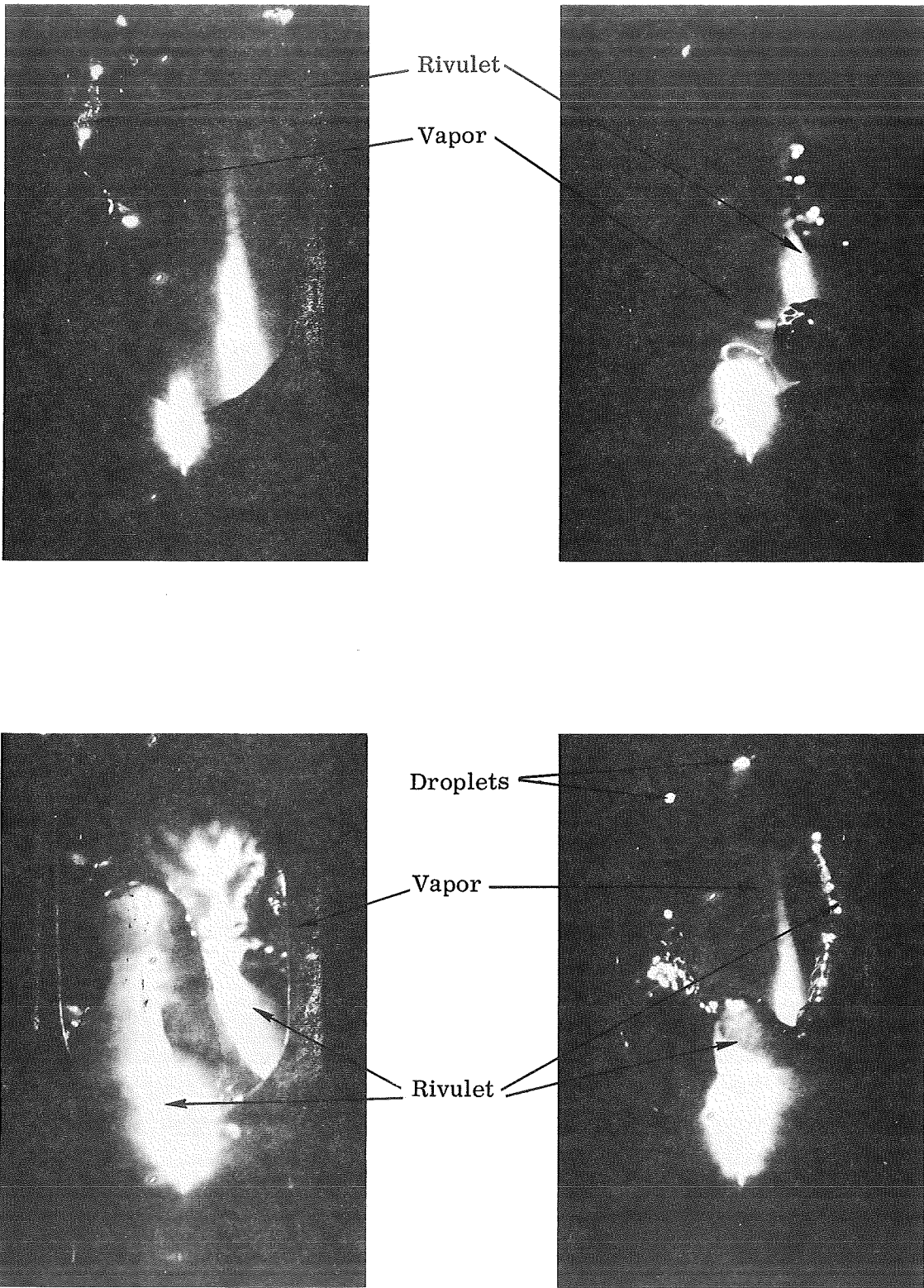
Figure 21. Helical forced flow boiling mercury, 13% vapor quality.
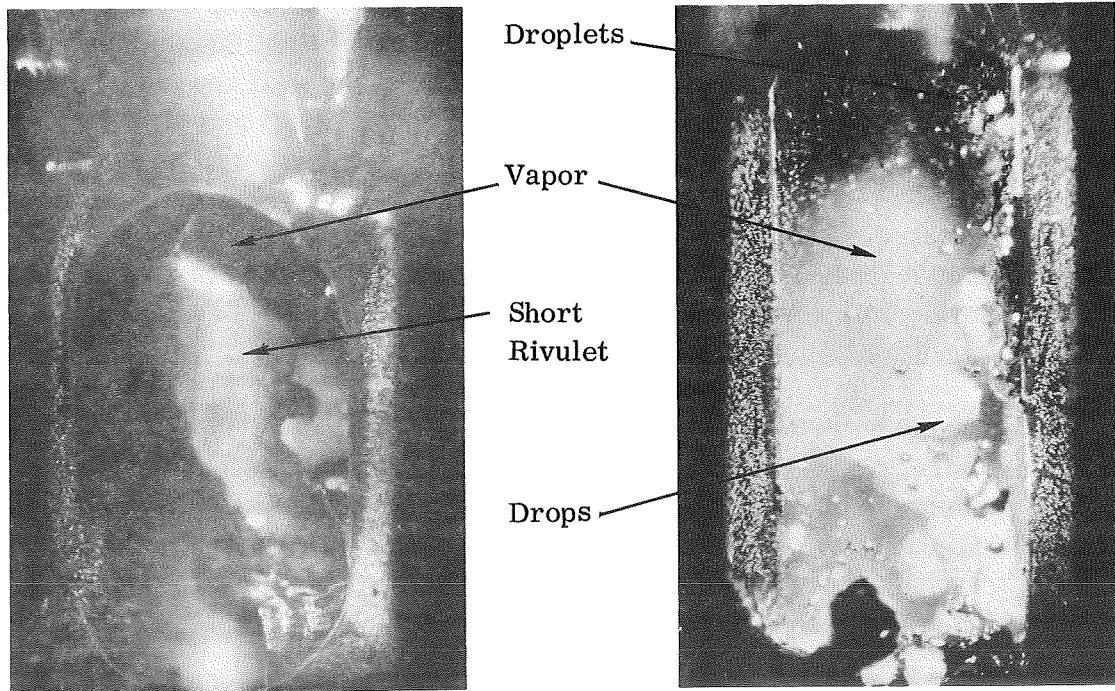
Rivulets

Vapor

Large Drop
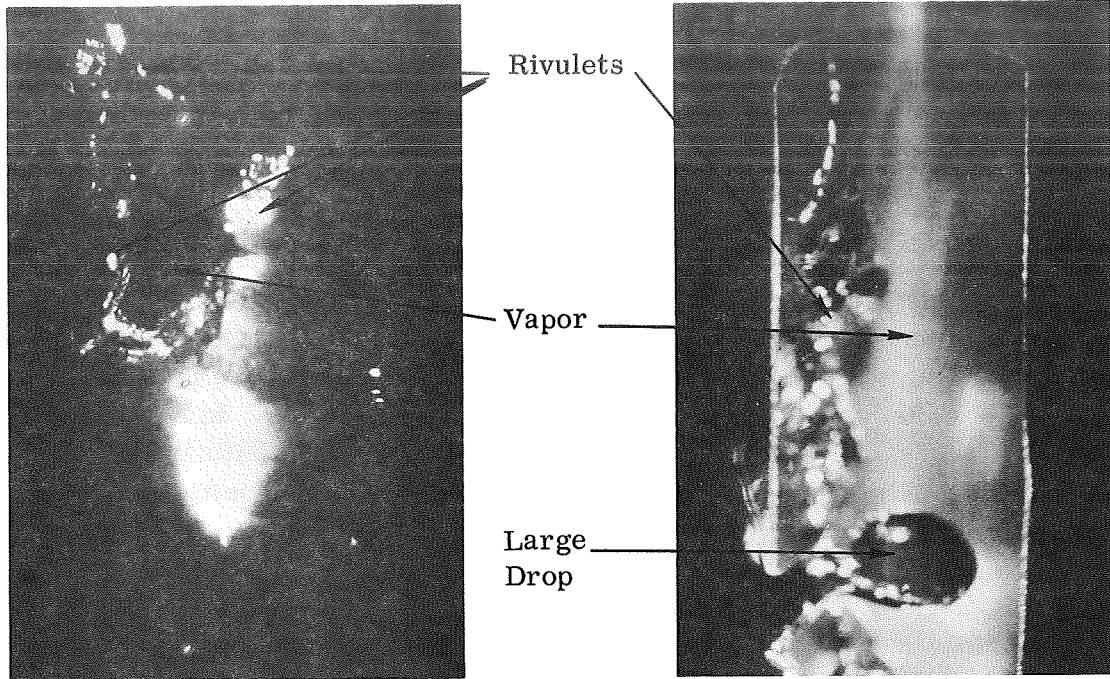
13% Vapor Quality, Helical Flow   11% Vapor Quality, Linear Flow

Droplets

Vapor

Short Rivulet

Drops

17% Vapor Quality, Helical Flow   20% Vapor Quality, Linear Flow

Figure 22.   Helical-linear radial phase distribution comparison.

to asperities) and spacings between obstructions or waves by ℓ. From the photographs of mercury phase distributions it is noted that the normalized obstruction heights, ϵ/R, and normalized obstruction spacings, ϵ/ℓ, can be as large as several tenths.

An analysis of an idealized multi-orifice roughness model is given in the Appendix (Note 2). From this model, it can be shown that for ϵ/R and ϵ/ℓ ratios of say 0.15 and Re equal to 10,000, the friction factor would be over ten times as large as the smooth pipe value. Although this example is hypothetical, the roughness ratios used are conservative in light of the photographic information cited above. The calculation suggests that the large experimental values for the friction factors in the SNAP-8 boiler tube entrance insert are not unreasonable. In Aerojet's report [8] it is shown that the insert friction factor increases significantly with mercury flow rate, suggesting that the increased vapor velocities and radial acceleration field at low mercury flow rates can be related to smoother liquid-vapor interfaces.

Vapor Superheat in a Boiler Tube and Liquid Carry-Over Reduction

A perfect helical flow insert at the exit of a boiler tube would keep the liquid component at the boiler wall in the form of a very thin annulus; at the 100 percent vapor quality point the liquid would be gone and no superheat would exist in the vapor. Beyond this point, the vapor would superheat and the radial temperature field is predictable by classical convection functions. If the flow insert is not perfect (because rotational flow is not sufficiently strong), film boiling rivulets and droplets would be present at the boiler exit. The dry regions of the wall and the contiguous vapor can be superheated (because of the relatively poor vapor heat transfer) while the vaporizing liquid droplets and rivulets can exist at near saturation temperature conditions.

In choosing an exit insert, it is desirable to create a flow pattern that keeps the liquid phase at the boiler wall where the phase-change proceeds at a high rate. Under these conditions, the liquid carry-over is small.

The question has been raised which of the two inserts, the twisted divider or the helical swirl wire, would be most effective as an exit insert. From the standpoint of getting a maximum number of droplets to be located at the wall, the twisted divider would be superior. From the standpoint of generating a maximum local radial acceleration field (as called for by the film boiling droplet flow model), the twisted divider is again superior.

IV. CONCLUDING REMARKS

1.   Oil leakage into the SNAP-8 mercury circuit can be transported into the boiler by two-component annular flow.

2.   Oil films in the boiler at design temperatures can be decomposed and the solid products deposited in the boiler.

3.   Decomposed oil deposits (and oxide deposits during earth-based operations) can significantly increase droplet vaporization lifetimes, cause changes in phase distributions in the boiler tube and reduce the corresponding boiling conductances.

4.   In order to guarantee no oil transport into the boiler, effective oil traps should be used in the systems.

5.   The heat transfer and pressure drop performance of SNAP-8 boilers can be defined by a number of idealized flow models (annular flow, wetted wall rivulet flow, film boiling droplet flow, slug flow, and vapor flow).

6.   Some approximate flow regime criteria have been developed which assist in defining which boiling regime is in operation.

V. APPENDIX

NOTE 1

AN ANALYSIS FOR SEPARATED FLOW IN
A MULTI-SLOT INSERT

From the shear stress-pressure drop and shear stress-strain equations one can obtain an equation for the velocity profile in the liquid layer, that is, for $r_0 < r < r_1$,

$$v = - \frac{1}{2 \mu_0} \frac{\partial p}{\partial x} \left(\frac{r^2}{2} - \frac{r_0^2}{2} \right) \tag{A-1}$$

Upon integrating from r_0 to r_1, the liquid mass flow rate, G_0, can be obtained,

$$G_0 = 2 \pi w_0 \left[- \frac{1}{4 \mu_0} \frac{\partial p}{\partial x} \left(\frac{r_0^4}{4} - \frac{r_1^4}{4} \right) + \frac{r_0^2}{4 \mu_0} \frac{\partial p}{\partial x} \left(\frac{r_0^2}{2} - \frac{r_1^2}{2} \right) \right] \frac{\beta}{2 \pi} \tag{A-2}$$

This relation represents one equation in two unknowns, namely r_1 and $(\partial p)/(\partial x)$, where

v, velocity profile in liquid layer

μ_0, liquid viscosity

$\frac{\partial p}{\partial x}$, two phase axial frictional pressure gradient in liquid and vapor

r, radial distance

r_0, inside radius of tube

r_1, radial distance to interface between two phases

G_0, liquid mass flow rate

w_0, liquid weight density

β, slot angle shown in Figure 15, radians

The pressure drop equation for turbulent gas flow in the irregular cross section is

$$\frac{\partial p}{\partial x} = \frac{\zeta \, w_1 \, V^2}{4R_h \, 2g}$$ (A-3)

where

ζ, Weisbach friction factor for interface between the two fluids

w_1, vapor weight density

V, mean vapor velocity

g, acceleration of gravity

R_h, hydraulic radius

In this analysis, it is postulated that the viscous liquid-turbulent vapor interface velocity, v_2, is small compared to the mean vapor velocity, V, and is thus neglected. The hydraulic radius definition is*

$$R_h = \frac{\text{flow area}}{\text{wetted perimeter}} = \frac{\pi \left(r_1^2 - r_2^2 \right) \frac{\beta}{2\pi} + \frac{\pi}{8} \left(\beta \, r_2 \right)^2}{\beta \, r_1 + 2 \left(r_1 - r_2 \right) + \frac{\pi}{2} \beta \, r_2}$$ (A-4)

where r_2 is the radial distance to the center of the arc defining the inner bound of the slot. The mean vapor velocity squared, V^2, can be expressed in terms of the continuity equation,

$$V^2 = \frac{G_1^2}{(\text{flow area})^2 \, w_1^2} = \frac{G_1^2}{w_1^2 \left[\left(r_1^2 - r_2^2 \right) \frac{\beta}{2} + \frac{\pi}{8} \left(\beta \, r_2 \right)^2 \right]^2}$$ (A-5)

---

*The geometrical bounds of the idealized slot are arcs of circles and radial segments. These arbitrary choices were made to simplify the algebra.

Substitution of Equations (A-4) and (A-5) into (A-3) yields

$$\frac{\partial p}{\partial x} = \frac{\zeta w_1}{8g} \frac{G_1^2 \left[\beta r_1 + 2 \left(r_1 - r_2 \right) + \frac{\pi}{2} \beta r_2 \right]}{w_1^2 \left[\left(r_1^2 - r_2^2 \right) \frac{\beta}{2} + \frac{\pi}{8} \left(\beta r_2 \right)^2 \right]^3} \qquad (A-6)$$

This expression is the second equation in two unknowns, r_1 and $(\partial p)/(\partial x)$.
Upon equating the pressure drop terms in Equations (A-2) and (A-6), there results

$$\frac{G_o}{2\pi w_o \left[-\frac{1}{4\mu_o} \left(\frac{r_o^4}{4} - \frac{r_1^4}{4} \right) + \frac{r_o^2}{4\mu_o} \left(\frac{r_o^2}{2} - \frac{r_1^2}{2} \right) \right] \frac{\beta}{2\pi}} =$$

$$\frac{\zeta w_1}{8g} \frac{G_1^2 \left[\beta r_1 + 2 \left(r_1 - r_2 \right) + \frac{\pi}{2} \beta r_2 \right]}{w_1^2 \left[\left(r_1^2 - r_2^2 \right) \frac{\beta}{2} + \frac{\pi}{8} \left(\beta r_2 \right)^2 \right]^3} \qquad (A-7)$$

or

$$\left[\frac{64}{\zeta \beta} \right] \left[\frac{g r_o \mu_1}{G_1} \right] \left[\frac{G_o \mu_o w_1}{G_1 \mu_1 w_o} \right] \frac{\left[(\rho^2 - \rho_2^2) \frac{\beta}{2} + \frac{\pi}{8} (\beta \rho_2)^2 \right]^3}{\left[\beta \rho + 2 (\rho - \rho_2) + \frac{\pi}{2} \beta \rho_2 \right]} = \left[-\frac{1}{2} (1 - \rho^4) + (1 - \rho^2) \right] \qquad (A-8)$$

where $\rho = r_1/r_o$ and $\rho_2 = r_2/r_o$. From Equation (A-7) it is possible to calculate r_1 (or ρ) the unknown liquid-vapor interface radius. This solution can be expressed symbolically as

$$\rho = \phi \left(\zeta, \beta, \rho_2, \frac{g r_o \mu_1}{G_1}, \frac{G_o \mu_o w_1}{G_1 \mu_1 w_o} \right) \qquad (A-9)$$

The two phase flow frictional pressure drop, $(\partial p)/(\partial x)$, can be generalized as follows. The frictional pressure drop in the slot, if completely filled with the vapor at flow rate, G_1 (no liquid present), would be

$$\left(\frac{\partial p}{\partial x}\right)_{\text{all vapor}} = \frac{\zeta_s w_1}{8g} \frac{G_1^2 \left[\beta r_o + 2(r_o - r_2) + \frac{\pi}{2} \beta r_2 \right]}{w_1^2 \left[\left(r_o^2 - r_2^2\right) \frac{\beta}{2} + \frac{\pi}{8} (\beta r_2)^2 \right]^3} \quad \text{(A-10)}$$

Upon dividing Equation (A-6) by (A-10), one obtains

$$\frac{\frac{\partial p}{\partial x}}{\left(\frac{\partial p}{\partial x}\right)_{\text{all vapor}}} = \frac{\zeta}{\zeta_s} \left[\frac{\beta \rho + 2(\rho - \rho_2) + \frac{\pi}{2} \beta \rho_2}{\beta + 2(1 - \rho_2) + \frac{\pi}{2} \beta \rho_2} \right] \left[\frac{(1 - \rho_2^2) \frac{\beta}{2} + \frac{\pi}{8} (\beta \rho_2)^2}{(\rho^2 - \rho_2^2) \frac{\beta}{2} + \frac{\pi}{8} (\beta \rho_2)^2} \right]^3 \quad \text{(A-11)}$$

where ρ is already known from Equation (A-9).

In order to estimate boiling heat transfer in the low vapor quality region in the boiler tube insert with wetted walls, three analyses have been made for the heat transfer in idealized, liquid layers contiguous to a wall. The liquid layers are either viscous in character or are liquid metals. The first model consists of a superheated liquid layer that is heated from the tube wall and loses heat from the liquid-vapor interface by evaporative heat transfer; heat transmission through the layer is achieved by conduction only. The second model is defined by a superheated liquid layer with wall heat addition and a uniform volume heat sink representing volume boiling. The third model is defined by a superheated liquid layer with wall heat addition and a volume heat sink that varies linearly from a maximum value at the wall to zero at the liquid-vapor interface. No liquid-vapor interface evaporative heat transfer occurs in the last two models.

The general differential equation that defines these three boundary value problems is

$$\bar{u} \frac{\partial t}{\partial z} = a \frac{\partial^2 t}{\partial y^2} - \frac{S}{\rho_\ell c_{p_\ell}} \quad \text{(A-12)}$$

where y is the transverse or radial dimension and z is the longitudinal dimension. In all cases, $(\partial t)/(\partial z) = 0$. For the first system $S = 0$, for the second system $S = S_m$, and for the third system $S = S_0 (1 - y/\delta)$ where $\delta = r_0 - r_1$. A temperature solution was derived for each case. Next, the difference between the wall and liquid-vapor interface temperatures was substituted into the Nusselt modulus equation. The results are given in Table II.

Momentum transfer equations for two phase flow in the insert have been derived in the previous section. From this theory, it is possible to calculate liquid layer thicknesses versus vapor quality. Consequently, for a given vapor quality the Nusselt modulus and heat transfer coefficient are determined.

TABLE II.

Nusselt Modulus Functions for Three Heat Transfer Models

Model	Nusselt Modulus
1. Heat loss at liquid-vapor interface	$\dfrac{2r_0}{\delta}$
2. Uniform volume heat sink	$\dfrac{4r_0}{\delta}$
3. Heat sink that varies linearly from maximum value at the wall to zero at the liquid-vapor interface	$\dfrac{6r_0}{\delta}$

FRICTION FACTOR FUNCTIONS FOR FLOW IN TUBES WITH LARGE SURFACE ROUGHNESSES

This study consisted of representing a rough wall duct by a multi-orificed tube (see Figure 23).* It was postulated that the total head loss in such a system is composed of frictional and orifice losses, namely,

$$h_L = \zeta \frac{L}{D} \frac{u_1^2}{2g} + nK \frac{u_1^2}{2g}$$

$$= \frac{L}{D} \left(\zeta + \frac{nK}{\frac{L}{D}} \right) \frac{u_1^2}{2g} \tag{A-13}$$

where

$$\zeta + \frac{nK}{\frac{L}{D}} = \zeta_{eq} \tag{A-14}$$

or

$$\frac{\zeta_{eq}}{\zeta} = 1 + \frac{nK}{\frac{L}{D}\zeta} \tag{A-15}$$

The ratio $\dfrac{n}{\frac{L}{D}}$ can be expressed as,

$$\frac{n}{\frac{L}{D}} = \frac{\frac{L}{\ell}}{\frac{L}{D}} = \frac{\frac{LD}{D\ell}}{\frac{L}{D}} = \frac{D}{\ell} = \frac{2\frac{\epsilon}{\ell}}{\frac{\epsilon}{R}} \tag{A-16}$$

---

*This model is predicated on the postulates that the orifices are very thin compared to ϵ and, further, ϵ is small compared to ℓ.
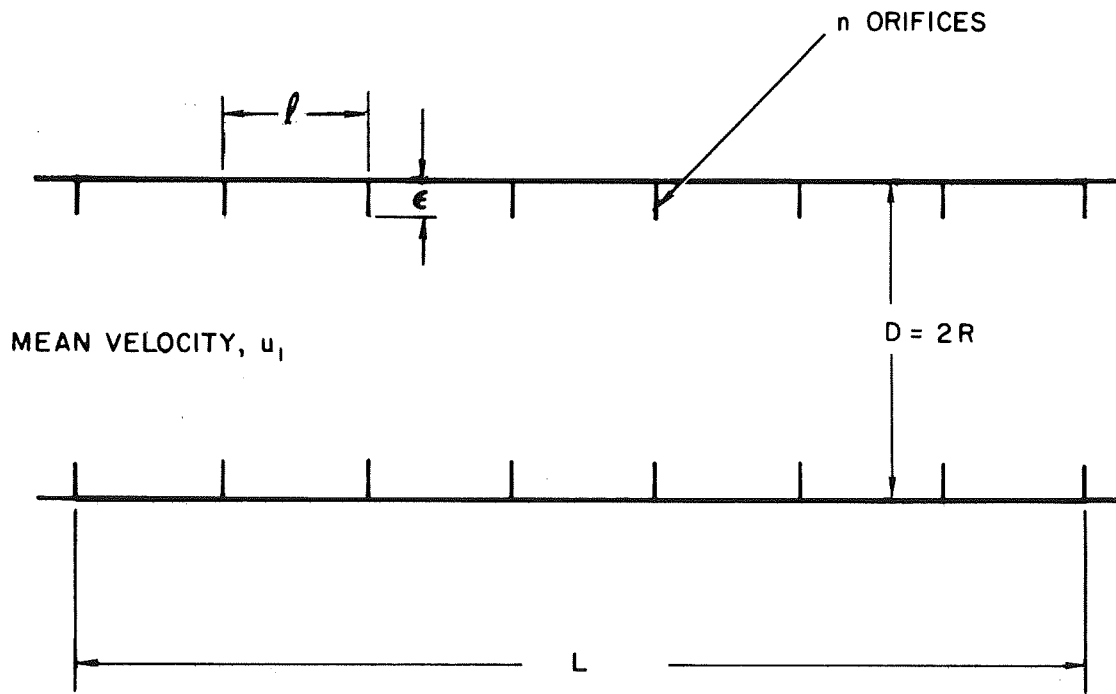
Figure 23. Multi-orifice roughness model.

The orifice loss coefficient, K, is postulated to be controlled by the classical sudden contraction coefficient,*

$$K = K_{sc} = \frac{R^4}{(R-\epsilon)^4} \left(\frac{1}{c} - 1\right)^2 = \frac{1}{\left(1 - \frac{\epsilon}{R}\right)^4} \left(\frac{1}{c} - 1\right)^2 \qquad (A-17)$$

where the constant, c, has been determined by experiment for various area ratios or values of ϵ/R (i.e., $c = f(\epsilon/R)$). The Weisbach friction factor, ζ, for smooth ducts is only a function of Reynolds number (Blasius equation, for example),

$$\zeta = f(Re) \qquad (A-18)$$

Substitutions of Equations (A-16), (A-17), and (A-18) into Equation (A-15) yields

$$\frac{\zeta_{eq}}{\zeta} = 1 + \frac{2\left(\frac{\epsilon}{\ell}\right)\left(\frac{1}{c\left(\frac{\epsilon}{R}\right)} - 1\right)^2}{\left(\frac{\epsilon}{R}\right)\left(1 - \frac{\epsilon}{R}\right)^4 \zeta}$$

$$= f\left(\frac{\epsilon}{\ell}, \frac{\epsilon}{R}, Re\right) \qquad (A-19)$$

Equation (A-19) is more general than the Karman-Prandtl equation used to represent the Nikuradse rough pipe data; the latter equation takes account of only the Reynolds number and the asperity height ratio, ϵ/R.

Equation (A-19) has been evaluated for a range of ϵ/R, ϵ/ℓ, and Re moduli; some of the results are shown in Figures 24 and 25. Note that for larger ϵ/ℓ ratios and ϵ/R ratios, very high equivalent friction factors can result.

---

*Only sudden contraction effects are included in the above orifice loss analysis. It was felt that this conservative representation would be more reasonable because many orifices are present in series, thus preventing complete contraction and expansion.
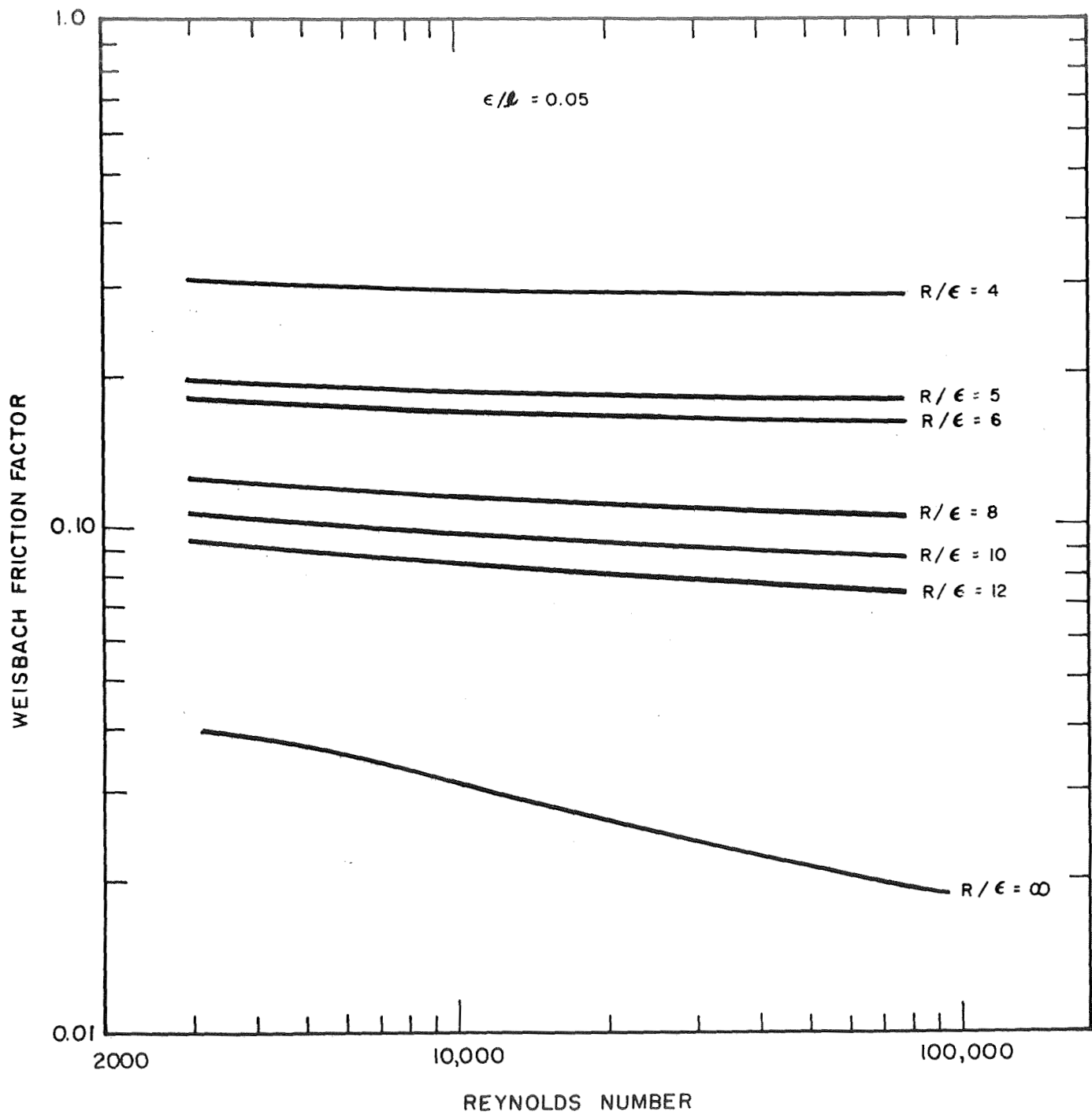
Figure 24.   Predicted friction factors for multi-orifice roughness model(ϵ/ℓ=0.05)
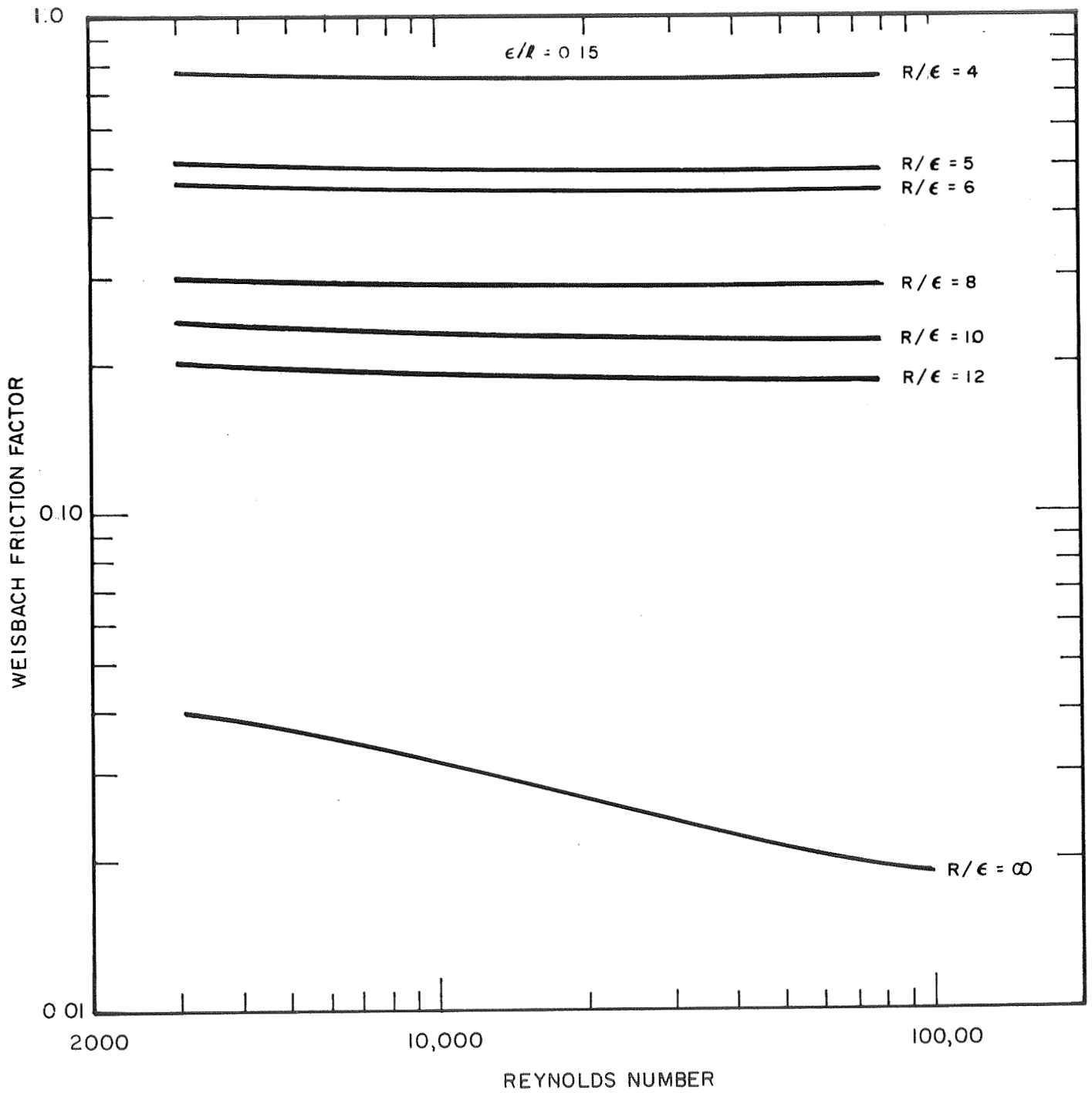
Figure 25. Predicted friction factors for multi-orifice roughness model (ϵ/ℓ= 0.15)

SYMBOLS

a, thermal diffusivity

A, a constant

$\bar{A}$, mean heat transfer area of drop

b_f, a shape factor for two-dimensional heat flow through the drop

c, constant in Equation (A-17)

c_{p_ℓ}, heat capacity of liquid in annulus

C, concentration of non-decomposed oil

C', concentration of non-decomposed oil expressed as a fraction

C'_o, concentration of non-decomposed oil expressed as a fraction at beginning of process

D, tube diameter (Figure 23)

f, fraction of the tube circumference covered by oil

f, function

F, fraction of the boiler tube area or circumference covered by a liquid rivulet

g, acceleration of gravity

G, rate of mercury vaporization

G_o, flow rate of annulus fluid

G_{o_f}, flow rate for an incomplete annulus

G_1, flow rate of core fluid

60

h, heat transfer conductance

h_L, head loss

k_i, thermal conductivity of deposit film

k_ℓ, thermal conductivity of liquid mercury

K, a reaction rate constant expressed as a fraction

K, orifice coefficient

K', a reaction rate constant that accounts for decomposition to a deposit film

K_{sc}, flow coefficient for sudden contraction

ℓ, spacing between obstructions or waves (Figure 23)

L, latent heat of vaporization of mercury

L, length in Figure 23

n, number of orifices

r, radial distance

r_o, tube inside radius

r_o, dimension in Figure 15

r_1, radius to annulus-core interface

r_1, dimension in Figure 15

r_2, radial dimension in Figure 15

R, inside tube radius (Figure 23)

R_H, hydraulic radius of slot (Figure 15)

S, volume heat source

t, coke layer thickness

t, temperature

t_{sat}, t_s, saturation temperature

t_w, wall or heat transfer surface temperature

T, temperature

$\bar{u}$, mean velocity of annular fluid

u_1, mean fluid velocity (Figure 23)

v, fluid velocity profile in mercury annulus of slot system

v_2, fluid velocity at liquid-vapor interface (Figure 15)

V, mean vapor velocity in core of slot system

V_o, oil volume added to system

w_d, density of liquid mercury

w_o, density of annulus fluid

w_1, density of core fluid

y, transverse coordinate

z, length of oil film

z, longitudinal coordinate

z_1, station or position at which coking begins

z_4, farthest lateral position along boiler tube at which oil is completely converted to coke

62

$\alpha,$ rivulet contact angle

$\alpha_c,$ critical contact angle

$\beta,$ angle in Figure 15

$\dfrac{\partial p}{\partial x},$ axial pressure gradient

$\delta,$ thickness of annulus

$\delta_i,$ deposit film thickness on boiler tube surface

$\delta_\ell,$ thickness for disc-shaped drop

$\delta_{\ell_o},$ thickness for disc-shaped drop at $\theta = 0$

$\epsilon,$ obstruction or wave height (Figure 23)

$\theta,$ time

$\theta_1,$ time at which coking begins at station or position 1

$\theta_\ell,$ droplet vaporization lifetime

$\theta_4,$ time at which all oil is decomposed to coke

$\mu_o,$ viscosity of annulus fluid

$\mu_1,$ viscosity of core fluid

$\zeta,$ Weisbach friction factor at the annulus-core interface

$\zeta_p,$ Weisbach friction factor for tube wall

$\zeta_s,$ Weisbach friction factor for the slot with all vapor

$\rho_\ell,$ mass density of liquid in annulus

$$N = \cfrac{\dfrac{\delta_i}{k_i}}{\dfrac{\delta_{\ell_o}}{2k_\ell}}$$

$$U = \cfrac{1}{\left(\dfrac{\delta}{k}\right)_\ell + \left(\dfrac{\delta}{k}\right)_i}$$

$$X = \frac{G_1\,\mu_1\,w_o}{G_o\,\mu_o\,w_1}$$

$$\rho = \frac{r_1}{r_o}$$

$$\zeta_{eq} = \zeta + \frac{nK}{L/D}$$

VI. REFERENCES

1. Poppendiek, H. F.; Feigenbutz, L. V.; Petrovits, Z. J.; Sabin, C. M.; Goddard, W. B.; "An Investigation of the Boiler Conditioning and Heat Transfer Characteristics in a Mercury-Tantalum System," GLR-65, Geoscience Ltd, July 1968.

2. Poppendiek, H. F.; Brown, J. F.; Sabin, C. M.; Feigenbutz, L. V.; "Final Report Investigation of SNAP-8 Boiler Conditioning and Heat Transfer Characteristics in a Mercury-Tantalum System," GLR-78, Geoscience Ltd, February 1970.

3. Poppendiek, H. F.; Greene, N. D.; Sabin, C. M.; Feigenbutz, L. V.; Mouritzen, G.; MacDonald, F. R.; Livett, R. K.; Chambers, J. E.; Schwartz, P. E.; Connelly, D. J.; Morton, W. A.; "Summary Report on High Acceleration Field Heat Transfer for Auxiliary Space Nuclear Power Systems," GLR-42, Geoscience Ltd, AEC Contract No. AT(04-3-409), SAN-409-29, January 1966.

4. Voorhies, Alexis, Jr., "Carbon Formation in Catalytic Cracking," Industrial and Engineering Chemistry, Volume 37, Part I, 1945.

5. Gunderson, R. C.; Hart, A. W.; "Synthetic Lubricants," Reinhold Publishing Company, 1962.

6. Sabin, C. M.; Poppendiek, H. F.; "Topical Report Heat and Momentum Transfer Model Studies Applicable to Once Through Forced Convection Potassium Boiling," GLR-71, Geoscience Ltd, GE Subcontract No. 037271952, NAS 3-9426 Boiler Development Program, pp 208 - 229, December 1969.

7. Poppendiek, H. F.; Greene, N. D.; Goddard, W. B.; Sabin, C. M.; "Investigation of Fundamental Mechanisms and Parameters that Influence Steady State and Transient Performance of Rankine Cycle Liquid Metal Systems," GLR-64, AEC Annual, Contract No. AT(04-3)-677, July 1, 1967 - June 30, 1968.

8. Sellers, A. J., "Topical Report on Thermal Design of SNAP-8 Tantalum-Stainless Steel Boiler," NASA CR 72760/Aerojet.